NUREG/CR-1835
R6, RB

Application of Lidar Techniques to Estimating Atmospheric Dispersion

Final Report

Manuscript Completed: November 1980
Date Published: December 1980

Prepared by
E. E. Uthe, W. B. Johnson

SRI International
333 Ravenswood Avenue
Menlo Park, CA 94025

Prepared for
Division of Reactor Safety Research
Office of Nuclear Regulatory Research
U.S. Nuclear Regulatory Commission
Washington, D.C. 20555
NRC FIN No. B6222
Under Contract No. NRC-04-77-147

8012290611

ABSTRACT

A new technique for collecting a large lidar data base appropriate for analyzing atmospheric diffusion parameters was developed, along with a new method for processing lidar data records on a large computer system (CDC-6400).

To test these new techniques, a two-week cooperative field program was conducted at the Idaho National Engineering Laboratory. Tracer gas and smoke releases were made by the National Oceanic Atmospheric Administration Air Resources Laboratory (NOAA/ARL), and lidar backscatter data were collected by SRI using the Mark IX mobile lidar system. All lidar data were reduced to the form of vertical cross-sections depicting the two-dimensional structure of tracer smoke at various distances downwind of the source.

These measured distributions of tracer smoke resulting from releases made simultaneously at sites near to and away from the Experimental Organic Cooled Reactor (EOCR) building provided data that could readily be used to determine building-wake effects. This analysis indicates that the presence of the building clearly enhances horizontal and vertical dispersion in the first 200 to 300 m of downwind travel. However, at downwind distances in the range of 300 to 500 m there is some evidence that vertical dispersion is suppressed in the building wake relative to that of the open-country release.

The techniques used for processing the lidar data collected during this project were shown to be feasible, but are not ideal for analysis of large data bases because of the expense involved in converting tape formats and generating an X-Y grid of backscatter values. The lack of an appropriate display system was also a problem. Based on this experience and a review of the latest digital hardware available, an improved data-handling approach has been devised, involving the addition of a new display memory with readback capabilities to the lidar data system. This method makes use of both small- and large-computer techniques, and is recommended for optimal processing and analysis of the large lidar data bases that are necessary in atmospheric dispersion studies.

CONTENTS

ILLUSTRATIONS

TABLES

ACKNOWLEDGMENTS

The authors are grateful for the valuable technical guidance and assistance rendered by Dr. Robert Abbey, the National Regulatory Commission (NRC) Project Officer, by Dr. Isaac Vanderhoven of the National Oceanic Atmospheric Administration Air Resources Laboratory (NOAA/ARL), and by Messrs. Ray Dickson, Gene Start, Jerry Sagendorf, and Norman Ricks of the NOAA/ARL Field Research Office, who cooperated fully in the joint field study at Idaho Falls.

We also acknowledge with thanks the assistance of several of our SRI colleagues in this project: Norman Nielsen and William Dyer, who participated in the field study; Charles Flohr, who helped with the data reduction; and Joyce Kealoha, who prepared the illustrations.

The lidar data examples used in Section III were obtained and prepared by SRI International under contract to the Electric Power Research Institute and are described in the following two final reports:

- Uthe, E. E. and W. B. Johnson, 1976: "Lidar Observations of Plume Diffusion at Rancho Seco Generating Station," EPRI NP-238 (SOA 75-316).
- Thuillier, R. H. and R. L. Mancuso, 1980: "Building Effects on Effluent Dispersion from Roof Vents at Nuclear Power Plants," EPRI NP-1380 (Project 1073-1).

The EPRI Project Manager for these two projects was Henry Till.

I INTRODUCTION AND BACKGROUND

A. General

In the event of an accidental release of radioactive effluent into the atmosphere from a nuclear power generating plant, the dosages received by persons downwind of the release depend on the transport, diffusion, deposition, and buoyant rise of the effluent. The range of dosages (or more specifically, the concentration distributions) that could result from such accidents are readily studied by releasing tracer material from a given location and measuring the tracer concentrations downwind with relatively high spatial resolution.

The project described in this report was part of an ongoing program of research in atmospheric dispersion conducted by the Office of Research of the Nuclear Regulatory Commission (NRC). The objective of this program is to verify dispersion models used to predict the concentration and spread of airborne radioactive effluents. Abbey (1975, 1976) described these NRC research activities in detail.

Lidar (laser radar) observations of tracer smoke plumes provide a relatively inexpensive means of collecting the required data. The lidar technique can obtain detailed measurements of tracer plume density distributions in the vertical over extended distances from the tracer source. For a general description of lidar principles and techniques, reference can be made to Collis and Uthe (1972).

B. Initial Feasibility Study at Rancho Seco Generating Station

During October 1975, a diffusion study using gas (SF_6) and smoke (oil fog) tracers was conducted at the Rancho Seco Generating Station near Sacramento, California, by the Air Resources Laboratory of the National Oceanic and Atmospheric Administration (NOAA). This field study was funded by the NRC as part of the research program discussed above.

During a portion of the Rancho Seco study, concurrent lidar measurements of the tracer smoke plume were conducted by SRI International under contract with the Electric Power Research Institute (EPRI). The measurements were made during the period 27-30 October, using the SRI Mark IX mobile lidar and its associated digital data processing and display system. [A description of the Mark IX system is given in the appendix; additional details are presented in Uthe and Allen (1975).]

The NOAA experiments involved periodically releasing tracer gas and smoke from points on or near the reactor containment structure for periods of approximately 30 minutes to 1 hour. The horizontal distribution of the tracer gas was measured by means of an array of air samplers situated at ground level on several arcs around the release point, out to a distance of 800 m. Five 46-m towers, spaced 30^{o} apart at a distance of 400 m, were also equipped with air samplers in an attempt to measure the vertical distribution of tracer gas. In addition, one tower was equipped with wind and air temperature sensors at five levels. The tracer smoke was observed visually by NOAA personnel and was used as a qualitative indicator of air motions.

The SRI lidar study was designed to take advantage of the availability of this tracer smoke by using the lidar observational techniques to map the smoke distribution in the vertical plane. In this way, the tracer smoke could be used to obtain quantitative measurements of plume diffusion.

The SRI Mark IX lidar system, installed in a mobile van complete with power-generating equipment, was used in this study to obtain detailed vertical cross sections of tracer smoke density. The system's real-time digital data acquisition, processing, and display equipment was used to generate pictorial displays of plume structure and to perform quantitative vertical concentration analyses.

This modest study at Rancho Seco demonstrated that the SRI Mark IX mobile lidar is useful for field studies of atmospheric diffusion. Although the lidar technique is not without limitations, it provides data on horizontal and vertical plume-density distributions with high temporal and spatial resolution. It is particularly effective above the ground, where it is difficult to make direct measurements using conventional techniques.

Details of the results of this study may be found in Uthe and Johnson (1976) or Uthe et al. (1979).

II OBJECTIVES AND APPROACH

A. Project Objectives

Subsequent to the Rancho Seco feasibility study, SRI International received a contract from the NRC Office of Nuclear Regulatory Research to develop and demonstrate methods for improving the use of the lidar technique for describing atmospheric dispersion characteristics, especially in the vertical, around nuclear power plants. Basically, the objectives of this program were to develop and demonstrate improved data recording and analysis techniques that would provide for:

- Uninterrupted recording over long time periods to obtain appropriate data for deriving time-averaged diffusion parameters.
- Efficient and cost-effective analysis of the large quantities of data that can be collected with the lidar technique.
- Transfer of data and diffusion parameters in a format appropriate for use by diffusion modelers.

B. Technical Approach

To accomplish the objectives of this project as stated above, work was undertaken in the four areas listed below:

- Development of improved methods for recording, display, and analysis of lidar data in terms of diffusion parameters.
- Application of the new analysis and display techniques to data previously obtained at Rancho Seco.
- Application of the new recording and display techniques during a field study conducted at the Idaho National Engineering Laboratory (INEL) near Idaho Falls, Idaho, in cooperation with the NOAA Air Resources Laboratory.
- Examination of the feasibility of extending the application of mobile lidar systems to other aspects of nuclear power plant effluent diffusion.

III DATA RECORDING AND ANALYSIS IMPROVEMENTS

A general description of the lidar equipment, experimental procedures, and data-analysis techniques is included in the appendix. In this section the specific tasks accomplished in this project are discussed.

A. Data Recording Improvements

Lidar data collected at Rancho Seco were recorded on a dual-DECTAPE unit manufactured by Digital Equipment Corporation (DEC). The original Mark IX lidar digital system employed this unit because it provided for high-reliability recording of lidar data on one DECTAPE, while a second DECTAPE could be used for storage of a very flexible real-time operating system (RT-11) designed to be run on the type of minicomputer (PDP-11) used in the lidar van. Details of the lidar digital data recording, processing, and display system and examples of its application have been presented by Uthe and Allen (1975).

Two major deficiencies resulting from use of DECTAPE as a recording medium were noted during the Rancho Seco tests (Uthe and Johnson, 1976). A single DECTAPE could record data from only 564 lidar firings. Therefore, after 564 observations, the lidar operations had to be suspended for about a 10-minute period while the recording tape was changed and the software reinitiated. On continuous runs, about one-third of the time was used to change tapes, and this could seriously affect the usefulness of data to be analyzed for diffusion parameters. In addition, because of their non-standard size and format, the DECTAPES could not be processed on off-line, large-computer systems to take advantage of the increased memory, speed, and subroutines for curve fitting and statistical analyses that are available with such systems.

For the lidar technique to become a routine method for measurement of vertical diffusion parameters, data recording must be accomplished on a magnetic tape system that allows for greater data storage and that offers compatibility with large computer systems. Accordingly, a nine-track magnetic tape recorder was installed in the lidar van and suitable software for data recording was developed. The magnetic tape unit allows for data storage of about 6000 lidar signatures as opposed to the previous 564 for DECTAPE. Software was also developed to decode the 16-bit words written by the PDP-11 lidar minicomputer in terms of the 60-bit word structure read by the SRI CDC-6400 computer system. This then provided a method for transferring the lidar data records to the CDC-6400 computer for utilization of more efficient analysis methods.

The new data-recording method was successfully applied during a field program conducted at the INEL from 31 October through 11 November 1977 in cooperation with the staff of the NOAA Air Resources Laboratory. The data and results obtained from the field program are presented in Section IV.

B. Data Analysis Improvements

A method was developed to allow for the efficient processing, in terms of vertical and horizontal diffusion parameters, of a large quantity of lidar data recorded on nine-track magnetic tape.

The first step was to streamline, refine, and document the computational procedures used to process lidar backscatter signatures in terms of an intensity-modulated TV-type display, as shown in Figure 1. Although the display technique was developed for use on the Rancho Seco diffusion study (Uthe and Johnson, 1976), the computer program for automatic profile analysis was not suitably refined and documented on this earlier project. Further, this procedure was available for use on DECTAPE data records only.

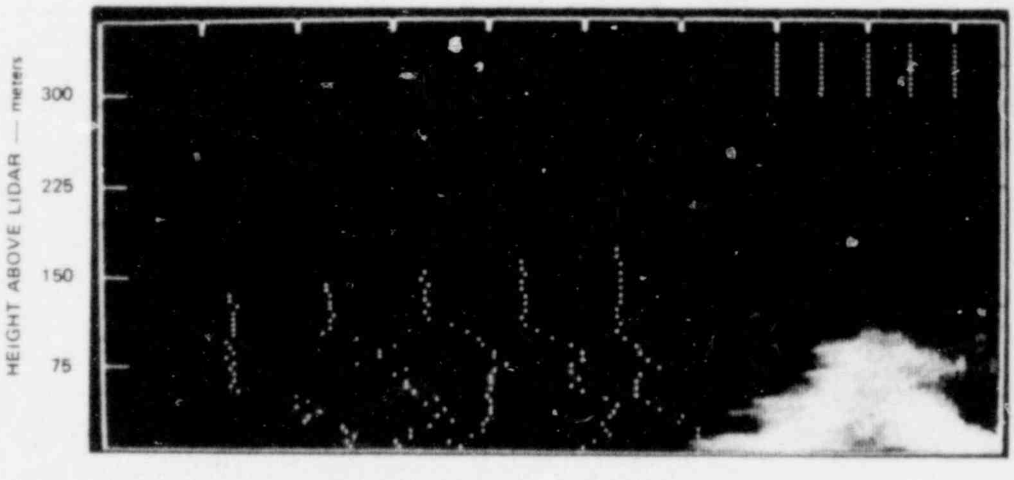

FIGURE 1 EXAMPLE OF COMPUTER-GENERATED VERTICAL PLUME DENSITY PROFILES

Lidar is located at lower left corner. The height and distance scale is 75 m/div. Plume vertical concentrations (relative to clear air with a scale of 10 dB/div) are plotted at the lower left and the horizontal position associated with each profile is plotted in the upper right.

To process lidar data for display as plume cross sections, as shown in Figure 1, an "overplotting" technique was developed to generate a polar plot on the available X-Y grid of TV brightness elements without using the relatively large computer times normally required to transform data between coordinate systems. (This technique is described in more detail in the appendix.)

After a plume cross-section has been generated, an X-Y grid of values is retained within the display memory. It would be convenient to perform calculations with these stored data, but unfortunately the display memory does not have the capability to be accessed by the minicomputer for readback of data. Also, the display stores only four-bit information, whereas the lidar data recorded on tape provide eight-bit information. Therefore, readdressing the data for the profile analysis as shown in Figure 1 requires a second reading from the magnetic tape unit and subsequent computer operations. Each of the vertical profiles displayed in Figure 1 requires about 5 minutes to generate.

The method for generating polar-scan plume cross sections described above was developed in a preliminary form for analysis of DECTAPE records collected at Rancho Seco. As discussed earlier, a nine-track magnetic tape unit was added to the lidar data system and was used during the field study conducted under this project at Idaho Falls. Consequently, the polar plotting programs had to be rewritten for analysis of nine-track magnetic tape records. While the data collection using nine-track magnetic tape recording was successful, the capabilities of the lidar data system to process these tapes were found to be limited. Basically, it was possible to plot the data in a polar format in real time, but it was not possible to perform the post-experiment profile analysis as shown in Figure 1.

This limitation resulted from two factors. First, the operating software for DECTAPE operations (DECTAPE driver) had to be retained, since the DECTAPE unit is still necessary to run the RT-11 operating system. Use of the new magnetic tape unit required additional computer memory to store the software for driving it, and this left insufficient memory to run the data analysis programs previously used with the DECTAPE records.

The second factor was even more serious. DECTAPE is a semi-random data storage device that uses a prestructured (block) format. Therefore, for the profile analysis, DECTAPE data can be effectively readdressed without performing extensive rewind and tape-search operations. On the other hand, the file-structured nine-track tape must be searched from the beginning of the tape for the data record of interest. This operation significantly adds to the data processing time (especially for data records near the end of the tape) and makes it too slow for processing large data bases. Therefore, processing of nine-track magnetic tape lidar records in terms of diffusion parameters is not feasible using the current capabilities of the Mark IX lidar digital data system.

Because of the limitations discussed above for processing nine-track magnetic tape records on the lidar data system, and because we expected that considerably more efficient computer processing could be performed on a large off-line computer system, our next major effort was to develop a methodology to analyze the lidar data records on the CDC-6400 computer located at SRI. The overall approach that was taken is illustrated in Figure 2.

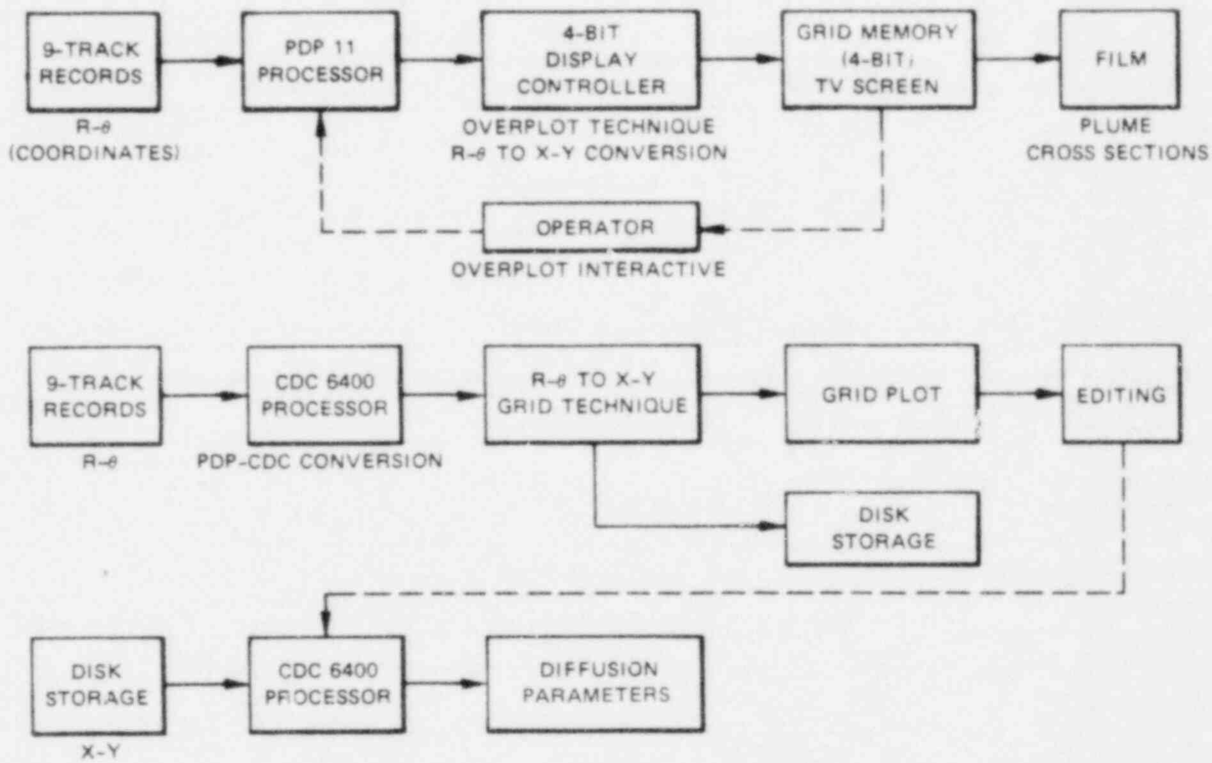

FIGURE 2 CURRENT PDP-11/CDC-6400 DATA-ANALYSIS APPROACH DEVELOPED FOR DIFFUSION PARAMETER COMPUTATION USING MARK IX LIDAR NINE-TRACK MAGNETIC TAPE RECORDS

First, a computer program was written to decode the 16-bit data words written by the PDP lidar minicomputer in terms of 60-bit words read by the CDC computer. This operation was found to be relatively expensive, and so a new tape was written that contained the decoded data and that could be efficiently processed by the CDC computer as many times as needed.

Unfortunately, a TV-type display system such as that used with the lidar minicomputer is not available on the CDC-6400 computer (or most other large-processor computer systems). However, both hardware and software are available on the CDC-6400 for generating both gray-scale and contour displays from an X-Y grid of data. Therefore, the next major effort on this study was to derive a method to transform the lidar elevation scan data (R-θ coordinates) into an appropriate X-Y data array. Since each lidar scan may contain as many as 50,000 data points, an efficient method must be employed to derive the X-Y grid-point array.

The basic steps that were used in deriving diffusion parameters from the lidar data are outlined below:

- Convert lidar backscatter signatures from digitizer counts ($C = -128$ to $+128$) to relative dB units by the expression $S = 0.181\ (C + 128)$, where the coefficient is determined periodically through calibration of the lidar receiver and log-amplifier circuits.
- Define the position of an X-Y mesh of grid points that overlays the R-θ grid-point array.
- Interpolate to determine S values at all grid points of the X-Y mesh. Each grid-point value is computed by linear interpolation using the two lidar signatures between which the grid point lies.
- Average the clear-air returns outside the plume to determine the background (clear-air) value, S_c, and subtract this value from all grid points to obtain normalized plume backscatter (S_p):

$$
\begin{aligned}
S_p &= S - S_c \\
&= 10 \log_{10} (\beta_p + \beta_c) - 10 \log_{10} \beta_c \\
&= 10 \log_{10} \left[(\beta_p + \beta_c)/\beta_c\right] ,
\end{aligned}
$$

  where β_p is backscatter from the plume particulates and β_c is backscatter from the clear air.
- Generate isolines of S_p using the X-Y grid-point array.
- Linearize the logarithmic Sp values to obtain values of relative plume density, D, defined as a normalized lidar backscatter ratio:

$$D \equiv \beta_p/\beta_c = 10^{S_p/10} - 1 .$$

- Time-integrate the resulting linear grid-point values obtained for a series of lidar elevation scans.

- Vertically integrate the time-integrated grid-point values to determine a cross-plume horizontal profile, and horizontally integrate the grid-point values to determine a cross-plume vertical profile.

- Compute diffusion parameters, σ_y and σ_z, by finding the nonlinear least-squares best fit of the Gaussian function to the vertically integrated horizontal profile and to the horizontally integrated vertical profile. (This procedure is described in more detail in the appendix.)

Standard SRI/CDC computer programs are available on the CDC-6400 that can generate two-dimensional displays from an X-Y grid of data points. One program generates a two-dimensional contour (isoline) analysis, and the other generates a two-dimensional gray-scale (dot pattern) picture. Figure 3 presents the output of the two approaches as applied to Scan No. 38 of the Rancho Seco data. Although the cost of producing these displays is considerably more than the gray-scale display generated by the lidar minicomputer system, a valuable by-product is the X-Y data-point matrix, which can be used for more efficient diffusion analysis.

Scan Nos. 36, 40, and 43 of the Rancho Seco data were chosen as a sample data set for use in developing software to compute time-integrated diffusion coefficients. The contour analyses for these scans, which were made at the same lidar viewing directions but at different times, are shown in Figure 4. For each cross section, the logarithmic backscatter values were converted to linear form and integrated in the horizontal for a cross-plume vertical profile and in the vertical for a cross-plume horizontal profile. A nonlinear least-squares routine is then applied to determine the best-fit Gaussian curve in a manner similar to that discussed in the appendix. The results of this analysis applied to the sample Rancho Seco cross sections are presented in Figure 5.

As illustrated by the data examples presented, using both the PDP and CDC computers in a coordinated manner provides for improved lidar data collection and analysis for determining values of atmospheric dispersion parameters. An alternative method of generating an X-Y grid of backscatter data by the lidar PDP-11 computer is recommended in Section V of this report. This proposed new method would greatly facilitate diffusion analyses of large lidar data bases by large computer systems.

This coordinated PDP/CDC computer analysis of lidar backscatter data in terms of time-integrated cross-plume diffusion has been applied to a portion (about 15 percent) of a large quantity of data collected on a project sponsored by the Electric Power Research Institute (EPRI) involving measurements of dispersion of tracer materials released near the Duane Arnold Energy Center. Examples are presented in Figures 6, 7, and 8. There are four parts to each of these figures:

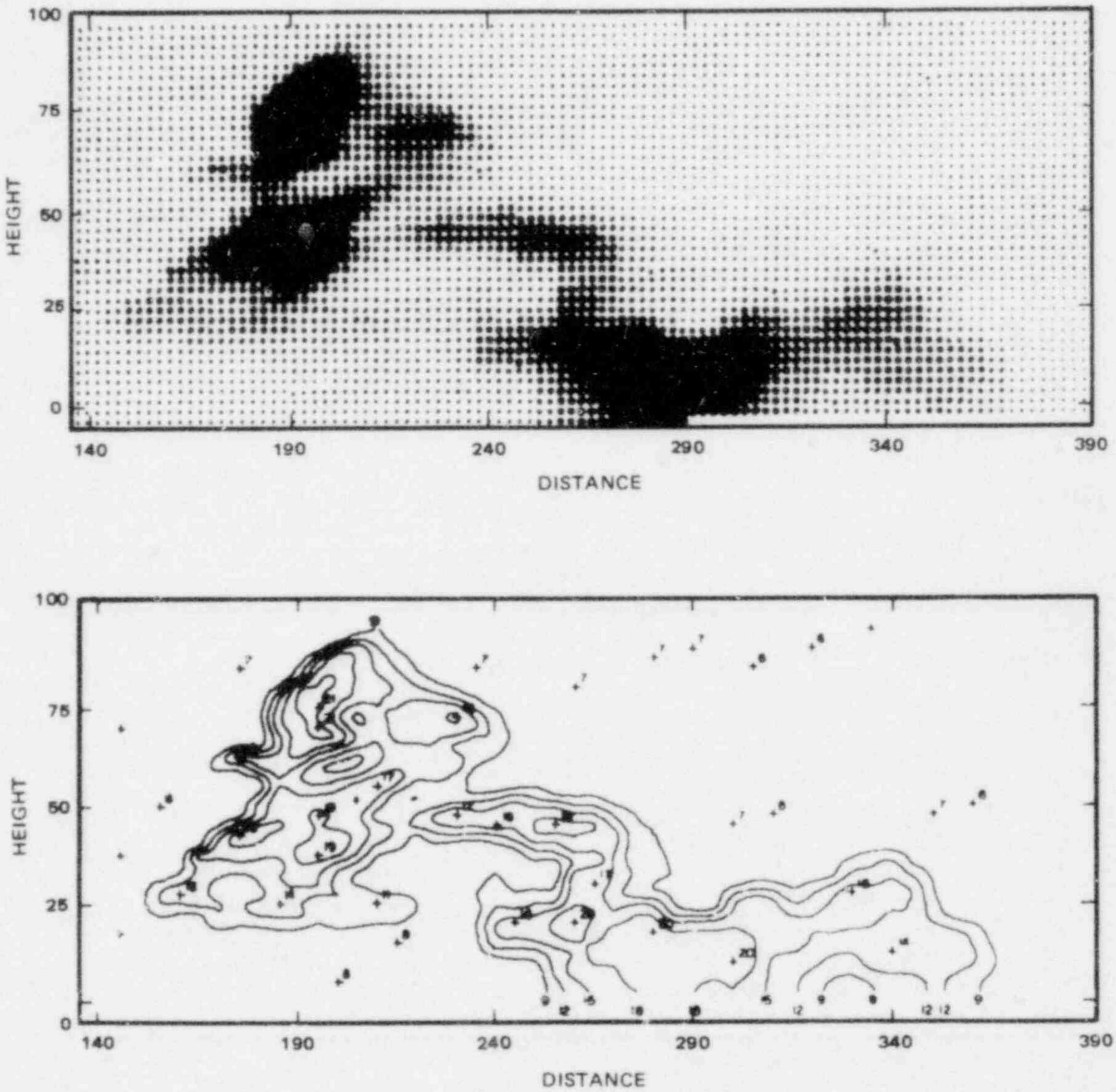

FIGURE 3 GRAY SCALE AND CONTOUR ANALYSIS OF A SMOKE TRACER PLUME (RANCHO SECO SCAN NO. 38) AS PROCESSED ON THE SRI CDC 6400 COMPUTER SYSTEM

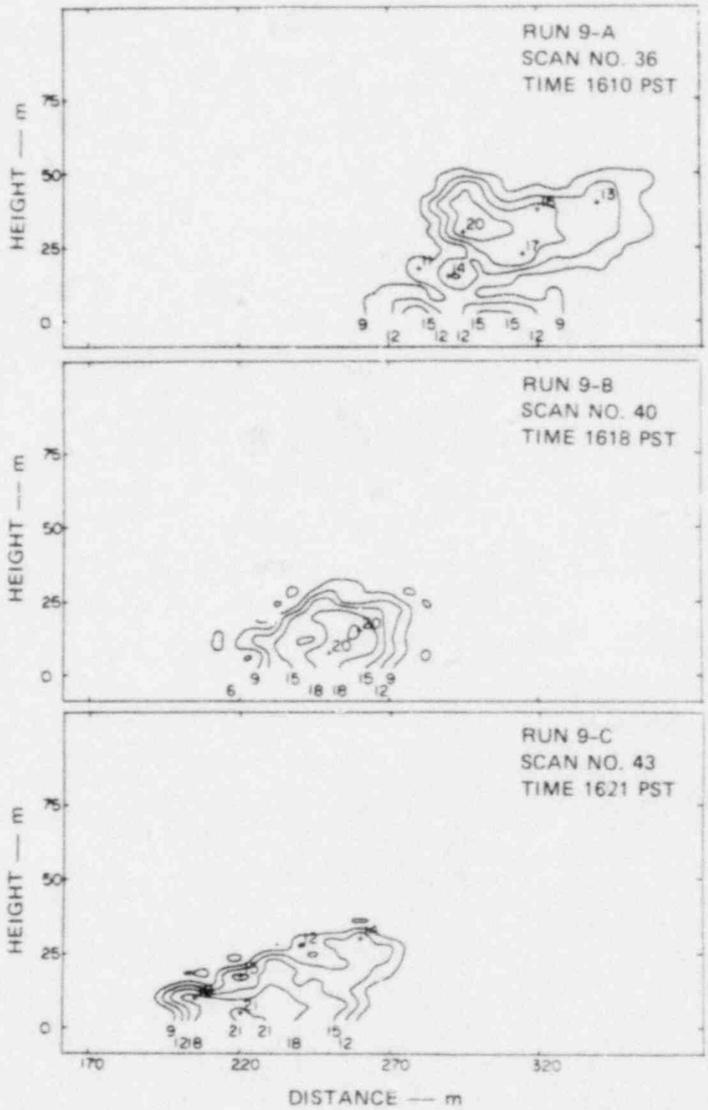

FIGURE 4 EXAMPLES OF COMPUTER-DRAWN CONTOUR PLOTS OF RELATIVE TRACER PLUME DENSITY (D) FOR RANCHO SECO RUN 9

Distance scale is offset to give greater detail; plume is getting closer to lidar as a function of time.

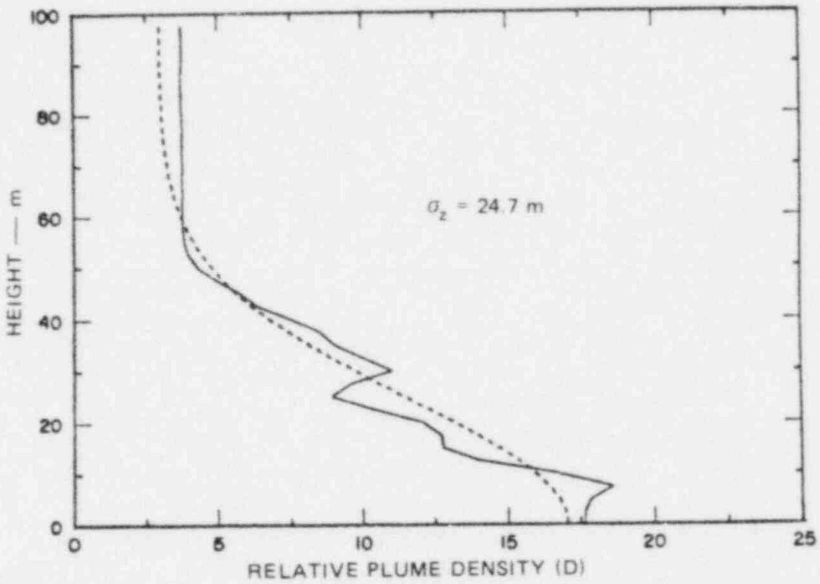

(a) VERTICAL PROFILE OF CROSS-WIND INTEGRATED RELATIVE PLUME DENSITY

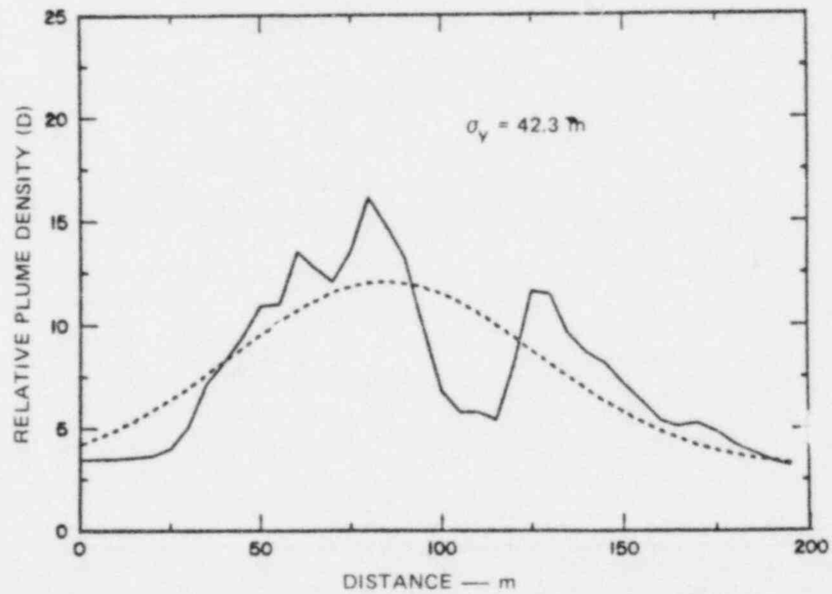

(b) CROSS-PLUME PROFILE OF VERTICALLY INTEGRATED RELATIVE PLUME DENSITY

FIGURE 5 TIME-AVERAGED RELATIVE PLUME DENSITY PROFILES FOR RANCHO SECO SCAN NOS. 36, 40, AND 43

See Figure 4.

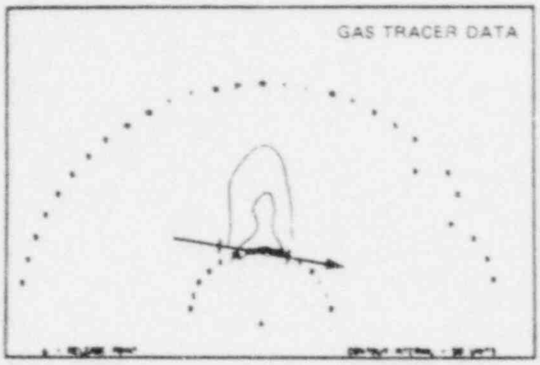

(a) PLAN VIEW – SF_6 CONCENTRATION – CONTOURS OF $\chi\bar{u}/Q$ (10^{-6} m^{-2})

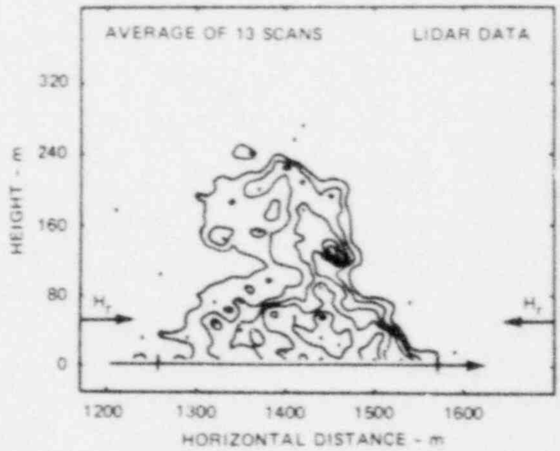

(b) VERTICAL CROSS SECTION - CONTOURS OF S_p INTERVAL = 1 UNIT; + = MAXIMUM POINT

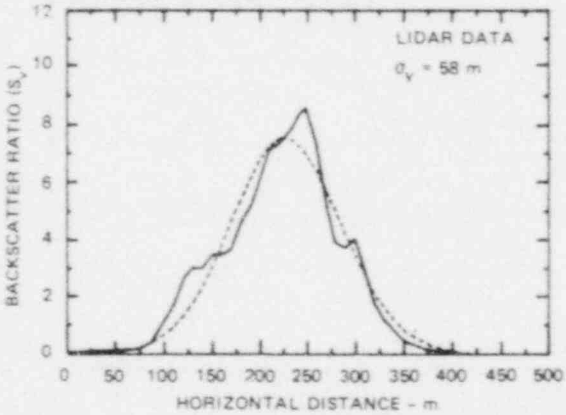

(c) VERTICALLY AVERAGED DISTRIBUTION OF D

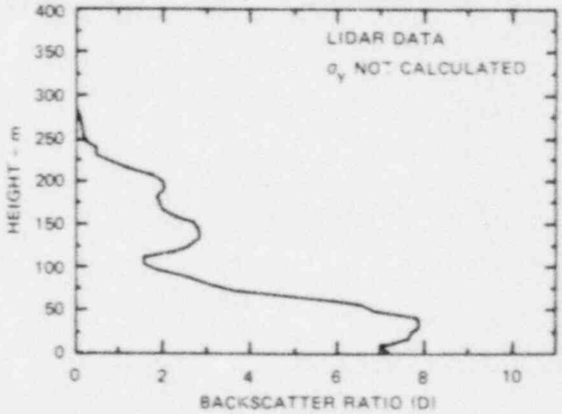

(d) HORIZONTALLY AVERAGED DISTRIBUTION OF D

NOTE: Path of lidar scanning plane; $\xrightarrow{H_r}$ height of reactor building above grade

FIGURE 6 CONTOUR PATTERN AND SPATIAL DISTRIBUTIONS OF HOURLY AVERAGED LIDAR AND GAS TRACER DATA FOR RUN 3 ON THE 300-m ARC

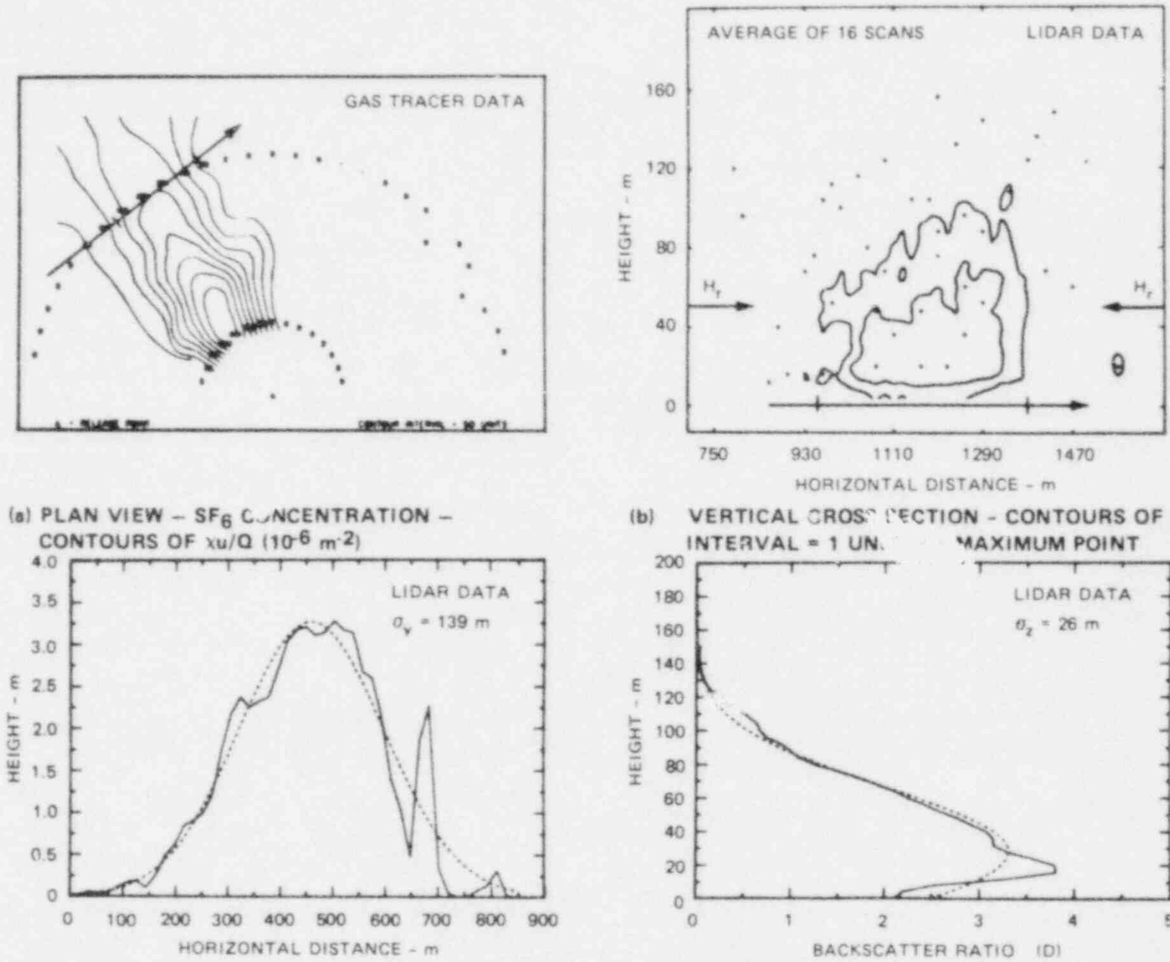

(a) PLAN VIEW – SF_6 C..NCENTRATION – CONTOURS OF $\chi u/Q$ (10^{-6} m^{-2})

(b) VERTICAL CROS' 'ECTION - CONTOURS OF S_p INTERVAL = 1 UN. ... MAXIMUM POINT

(c) VERTICALLY AVERAGED DISTRIBUTION OF D

(d) HORIZONTALLY AVERAGED DISTRIBUTION OF D

NOTE: Path of lidar scanning plane; H_r height of reactor building above grade

FIGURE 7 CONTOUR PATTERN AND SPATIAL DISTRIBUTIONS OF HOURLY AVERAGED LIDAR AND GAS TRACER DATA FOR RUN 23 C.N THE 1000-m ARC

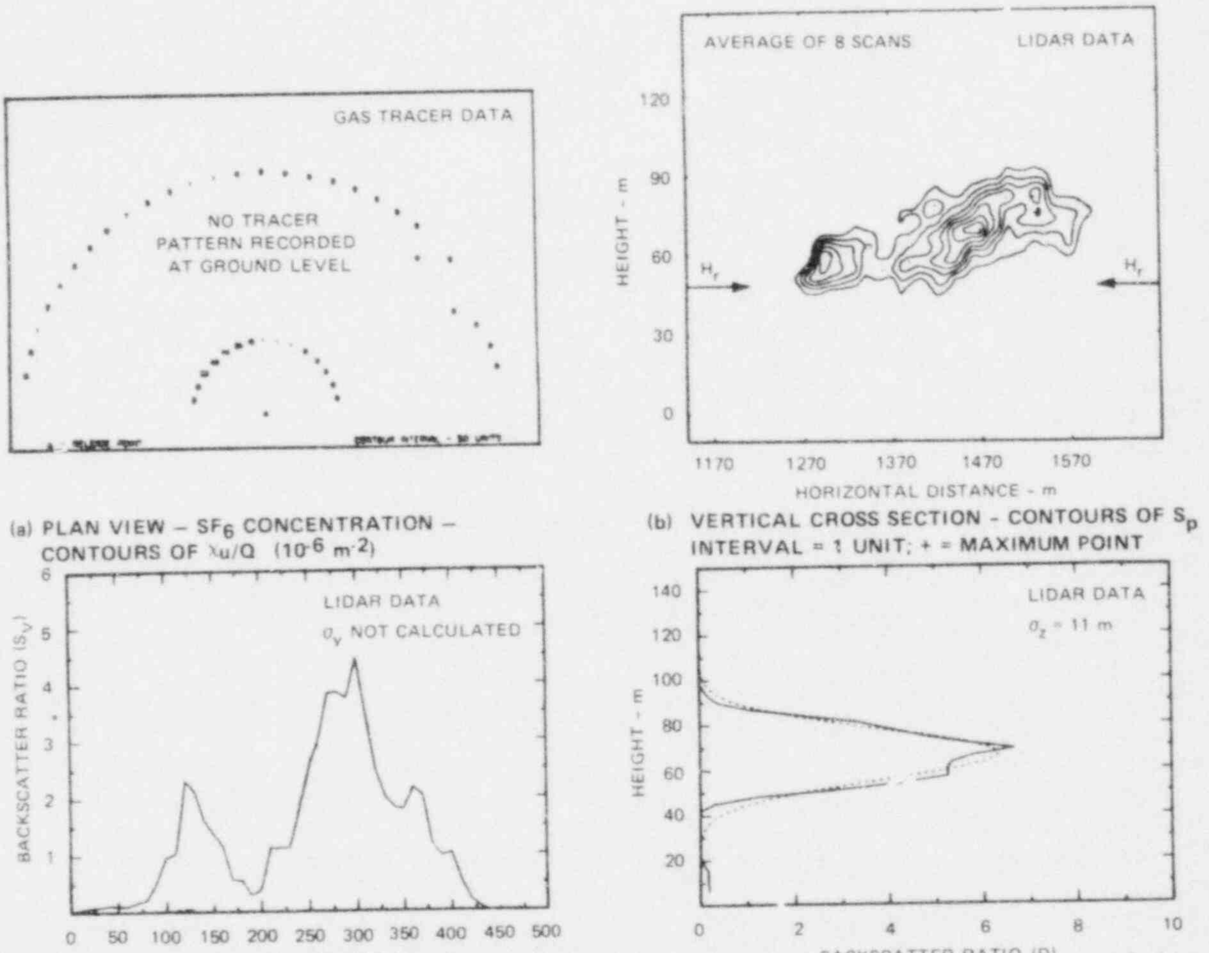

(a) PLAN VIEW – SF_6 CONCENTRATION – CONTOURS OF $\chi u/Q$ (10^{-6} m^{-2})

(b) VERTICAL CROSS SECTION - CONTOURS OF S_p INTERVAL = 1 UNIT; + = MAXIMUM POINT

(c) VERTICALLY AVERAGED DISTRIBUTION OF D

(d) HORIZONTALLY AVERAGED DISTRIBUTION OF D

NOTE: —+—+— Path of lidar scanning plane; $\xrightarrow{H_r}$ height of reactor building above grade

FIGURE 8 CONTOUR PATTERN AND SPATIAL DISTRIBUTIONS OF HOURLY AVERAGED LIDAR AND GAS TRACER DATA FOR RUN 30 ON THE 300-m ARC

(a) A contour analysis (horizontal cross section) of near-ground SF_6 tracer gas concentrations as measured using an array of air samplers located as indicated in the figure.

(b) A contour analysis (vertical cross section) of relative plume density (D) in the vertical plane as measured with the lidar.

(c) A horizontal profile of the vertically averaged relative plume density (D).

(d) A vertical profile of the horizontally averaged relative plume density (D).

It should be noted that all of these data represent 1-hour averages. To obtain this time integration, at least eight lidar elevation scans were averaged for each case, as indicated in the (b) portions of the figures. Where appropriate, a nonlinear least-squares Gaussian fit to the density distribution was made and is indicated by a dashed line in the (c) and (d) portions of the figures, and the standard deviation (σ) with respect to distance is provided.

Also, to clarify the relationship between the plan-view gas-tracer contour pattern and the lidar contour pattern in the vertical plane, the direction of lidar scanning is indicated by an arrow which contains tick marks indicating the lateral extent of the lidar contour pattern. The ticked arrow indicator appears on both the gas tracer and lidar patterns for cross-referencing. Zero height on the ordinate of the lidar contour pattern refers to the actual elevation of the lowest lidar pulse at the individual site of scanning. Lidar zero elevation may differ slightly from ground elevation at some points by virtue of the slightly undulating terrain. In some cases it will be noted that lidar information begins above the lidar zero elevation. This data loss is due to occasional, unavoidable attenuation of the lowest lidar pulses by objects such as trees and bushes.

It is clear from these data examples, as well as from those presented earlier, that lidar data are of value in dispersion studies of this sort. Several of the features shown by the lidar data could not have been observed by any other technique. For example, Figure 6 shows that an assumption of Gaussian-type vertical diffusion would not be valid in this case. Figure 7 indicates that the plume maximum concentration occurs 20 to 30 m above the ground. Figure 8 shows that the plume is fully elevated. None of these important plume features were revealed by the ground-based tracer-sampling network.

IV FIELD PROGRAM

A. Description of the Experiment

A two-week field study was conducted at the Idaho National Engineering Laboratory during the period 31 October - 11 November 1977. Measurements were made with the SRI Mark IX mobile lidar system in cooperation with the Idaho Falls Field Office of the NOAA Air Resources Laboratory (ARL-ID). The ARL-ID personnel coordinated the measurement program and generated smoke tracers, in addition to making gas tracer releases and measurements at surface level for some of the tests. The NOAA Wave Propagation Laboratory also participated in the field study by measuring winds and turbulence with their CO_2 Doppler lidar system.

The experiments were designed to investigate the feasibility of using lidar technology to obtain diffusion measurements in the vertical plane. The experiments were conducted at two field sites. One site was characterized by an abandoned reactor building (EOCR), and the other by an array of surface and tower-mounted tracer samplers (GRID III) operated by ARL-ID.

At the EOCR site, experiments were designed and conducted in a manner to:

- Ascertain the effects of a building structure on the diffusion of tracers released near ground level, and quantify to the extent possible.
- Determine the sensitivity of the building-wake effects to release height by making both vent (building-top) and stack (above-building-top) releases.

The experiments at the GRID III site were designed and conducted in a manner to:

- Validate lidar-derived diffusion parameters by comparison with results obtained from tracer-gas measurements.
- Extend the results to downwind distances for which tracer gases were not being sampled.

For each experiment, a smoke tracer plume was generated and the Mark IX lidar van was located at an appropriate site for making vertical cross sections through the smoke plume. Cross sections at several downwind distances were made by changing the azimuth viewing direction of the lidar system. Table 1 presents a summary of the Mark IX data collection

Table 1

SUMMARY OF LIDAR OBSERVATIONS OBTAINED DURING INEL FIELD STUDY
(31 October -- 11 November 1977)

Date	Run No.	Site No.*	No. of Cross Sections	Test Description
11-1-77	1	1-1	6	Smoke Pot--Stack Release
11-2-77	2	1-2	47	Oil Fog--Ground Level
11-2-77	3	1-3	14	Oil Fog--Ground Level
11-2-77	4	1-2	29	Oil Fog--Ground Level
11-2-77	5	1-3	37	Oil Fog--Ground Level
11-3-77	6	1-4-5	6	Smoke Pot Out of Stack
11-3-77	7+	1-4/5	10	Smoke Pot Out of Stack
11-3-77	8+	1-4/5	22	Smoke Release--Top of Building
11-3-77	9+	1-4/5	25	Oil Fog Behind Building
11-3-77	10	1-5	23	Oil Fog at Distance--Smoke Pot at Building
11-3-77	11	1-5	9	Oil Fog at Distance--Smoke Pot at Building
11-4-77	12	2-6	63	Grid Test--Oil Fog
11-8-77	13	2-7	24	Grid Test--Oil Fog
11-9-77	14	2-7	61	Grid Test--Oil Fog
11-10-77	15	2-7	43	Grid Test--Oil Fog
11-11-77	16	1-8	45	Oil Fog at Distance--Smoke Pot at Building
11-11-77	17	1-8	38	Oil Fog at Distance--Smoke Pot at Building

* Site number is given by prefix denoting reactor (1) or sampling grid (2) site and a suffix denoting the lidar site as keyed to a map of the area

+ Runs 7, 8, and 9 were between Sites 4 and 5.

operations. The lidar site numbers identified in Table 1 are indicated on the EOCR and GRID III maps shown in Figures 9 through 11.

B. Data Reduction and Presentation

As shown in Table 1, a total of 502 lidar cross-sectional scans were collected during the experiments at INEL. All of these lidar scans were processed into electronics and photographic images ("gray-scale displays") depicting vertical plume structure in the format shown in Figure 1. However, as discussed earlier, because of limitations in the Mark IX digital data system when using nine-track magnetic tape records, it was not feasible to derive plume density profiles as shown in Figure 1. The lidar cross sections were analyzed in terms of horizontal plume dimensions relative to the lidar position and these data were plotted on maps of the EOCR and GRID III sites to illustrate horizontal plume structure downwind of the smoke source. For example, Figure 12 presents plume positions observed during a relatively short run (Run 11) that consisted of two simultaneous smoke releases, one at ground level near the reactor building, and another at ground level in open country, approximately 200 m away in the crosswind direction from the building. Figure 13 presents the lidar cross sections collected during Run 11. In addition to Run 11, the dual-release approach also was used in Runs 10, 16, and 17 (see Table 1). Lidar cross sections for these runs are presented in Figures 14, 15, and 16.

In these figures, the cross sections at the larger azimuth angles are nearer to the smoke sources. These close-in cross sections, such as No. 11-1 (Figure 13), clearly indicate that the initial horizontal and vertical dispersion is considerably greater for the smoke released in the building wake (plume on left) than for that released away from the building (plume on right). However, at longer downwind distances, this does not always appear to be the case, at least not for vertical dispersion.

The influence of the building on vertical dispersion was investigated qualitatively by carrying out a picture-by-picture comparison of the heights of the two smoke plumes in each cross section. Values of a vertical dispersion comparison factor (F) were defined as follows:

$$\text{If } A_v > B_v \ , \quad F \equiv 2$$

$$A_v = B_v \ , \quad F \equiv 1$$

$$A_v < B_v \ , \quad F \equiv 0$$

where A_v = vertical extent of plume released away from the building

B_v = vertical extent of plume released near the building.

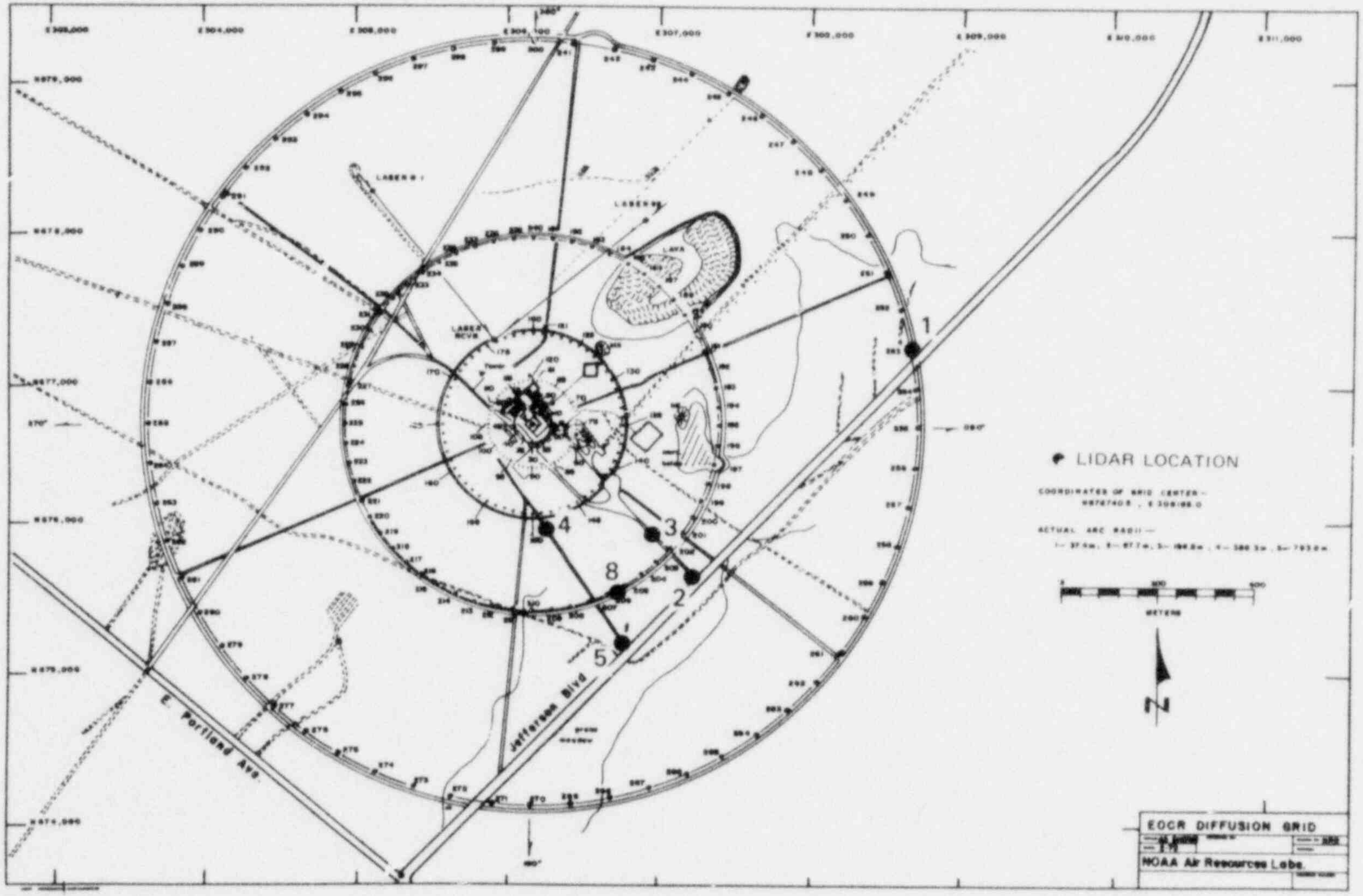

FIGURE 9 MAP OF THE EOCR SITE SHOWING LIDAR LOCATIONS USED DURING THE FIELD STUDY

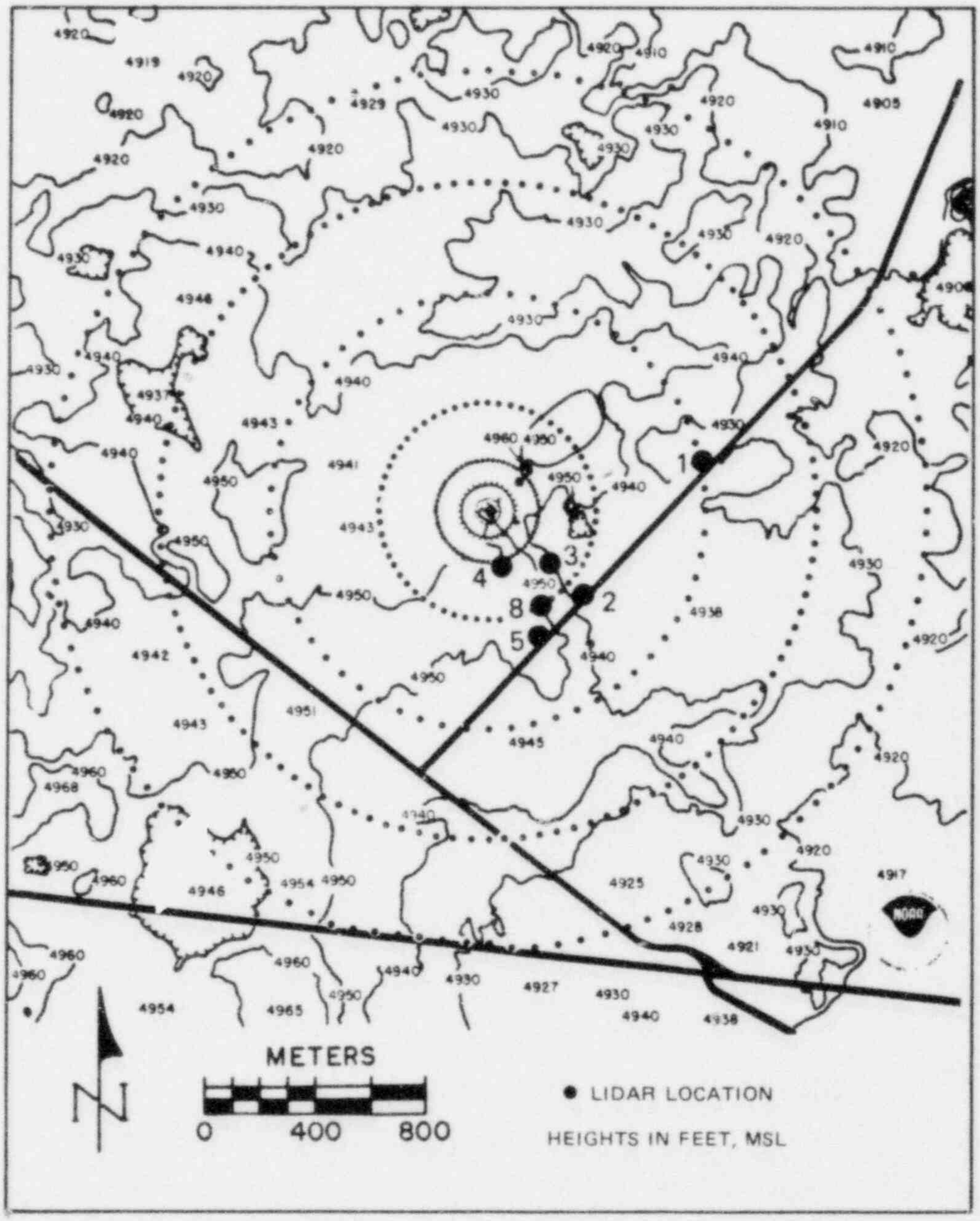

FIGURE 10 TOPOGRAPHICAL MAP OF THE EOCR SITE SHOWING LIDAR LOCATIONS USED DURING THE FIELD STUDY

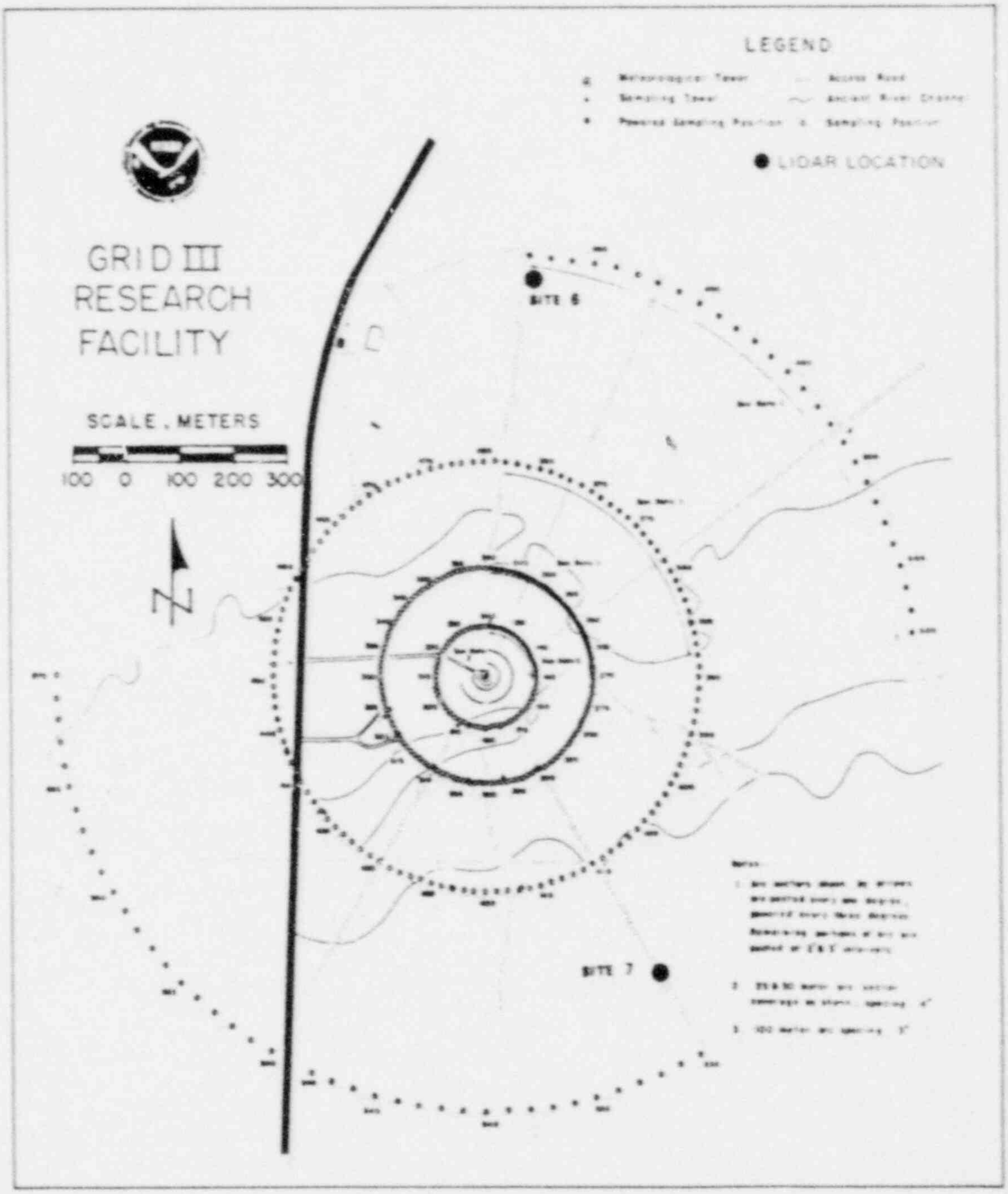

FIGURE 11 MAP OF THE GRID III SITE SHOWING LIDAR LOCATIONS USED DURING THE FIELD STUDY

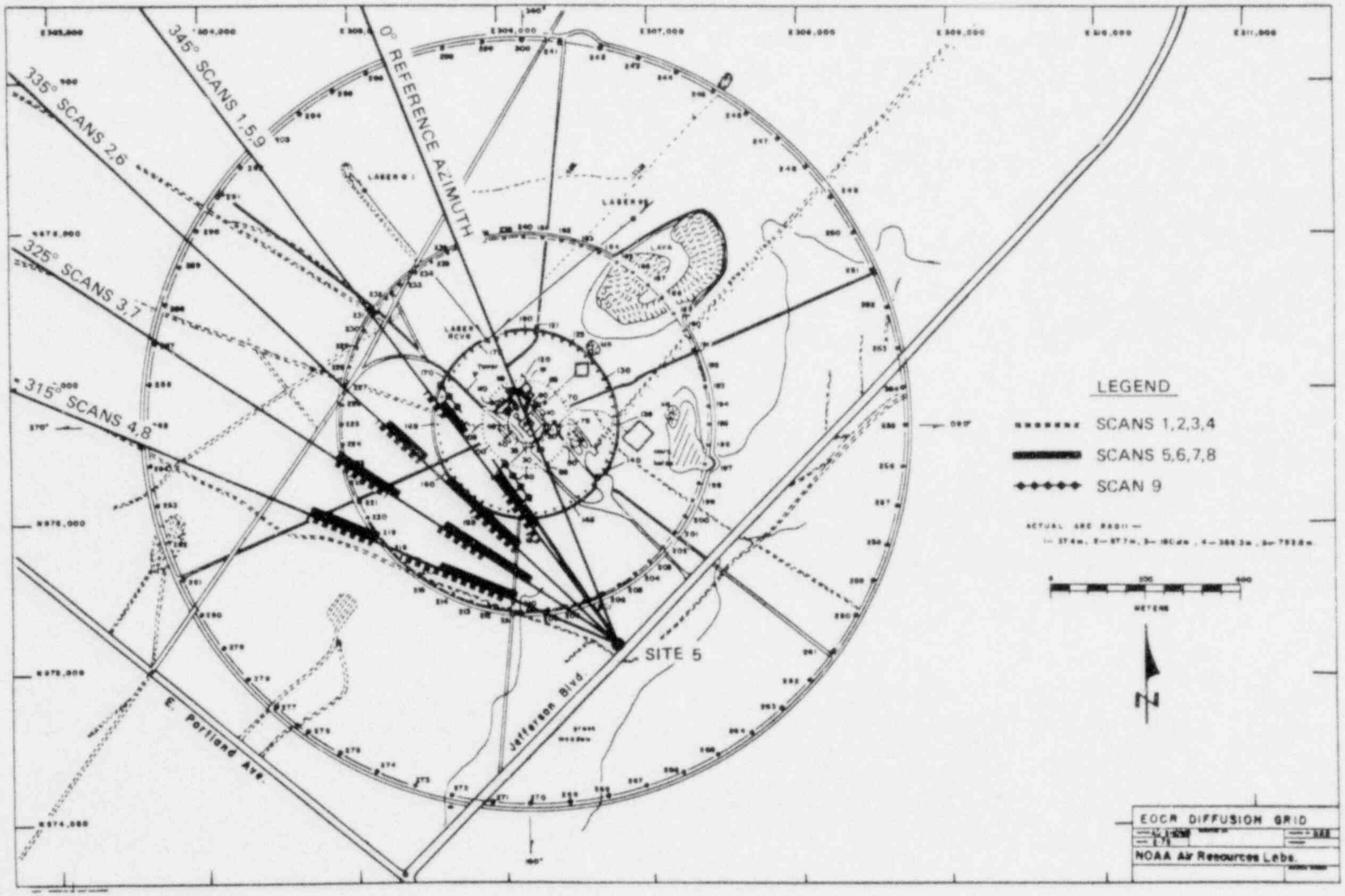

FIGURE 12 LIDAR-OBSERVED PLUME POSITIONS DURING RUN 11 AT THE EOCR SITE ON 3 NOVEMBER 1977

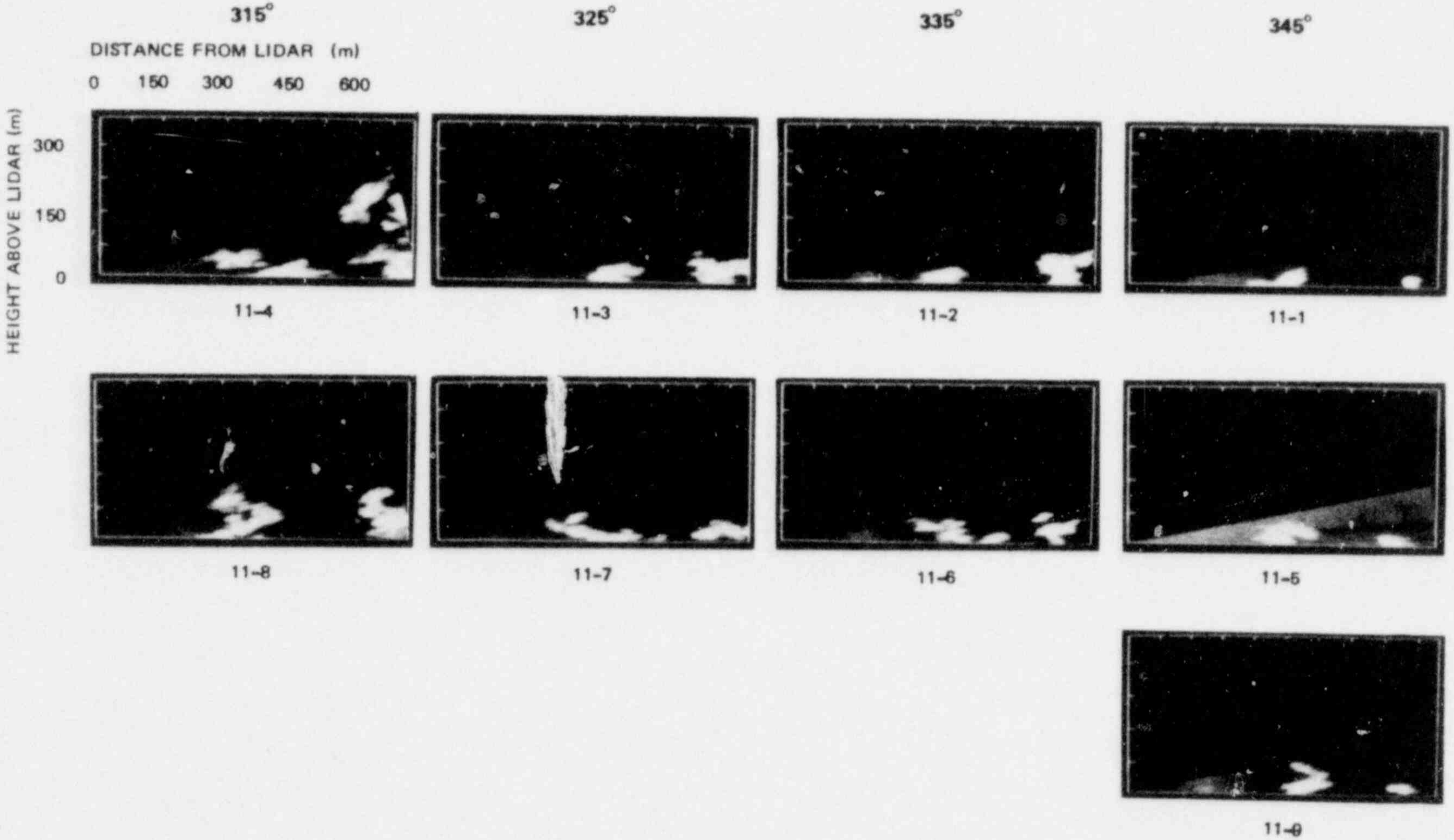

FIGURE 13 LIDAR VERTICAL CROSS SECTIONS OF TRACER SMOKE PLUMES RELEASED CONCURRENTLY NEAR THE EOCR BUILDING (PLUMES ON LEFT SIDE OF PICTURES) AND IN OPEN COUNTRY (PLUMES ON RIGHT SIDE OF PICTURES) FOR RUN 11

Scans at several lidar pointing (azimuth) angles are shown; the larger angles give data closer to the release points (see Figure 12).

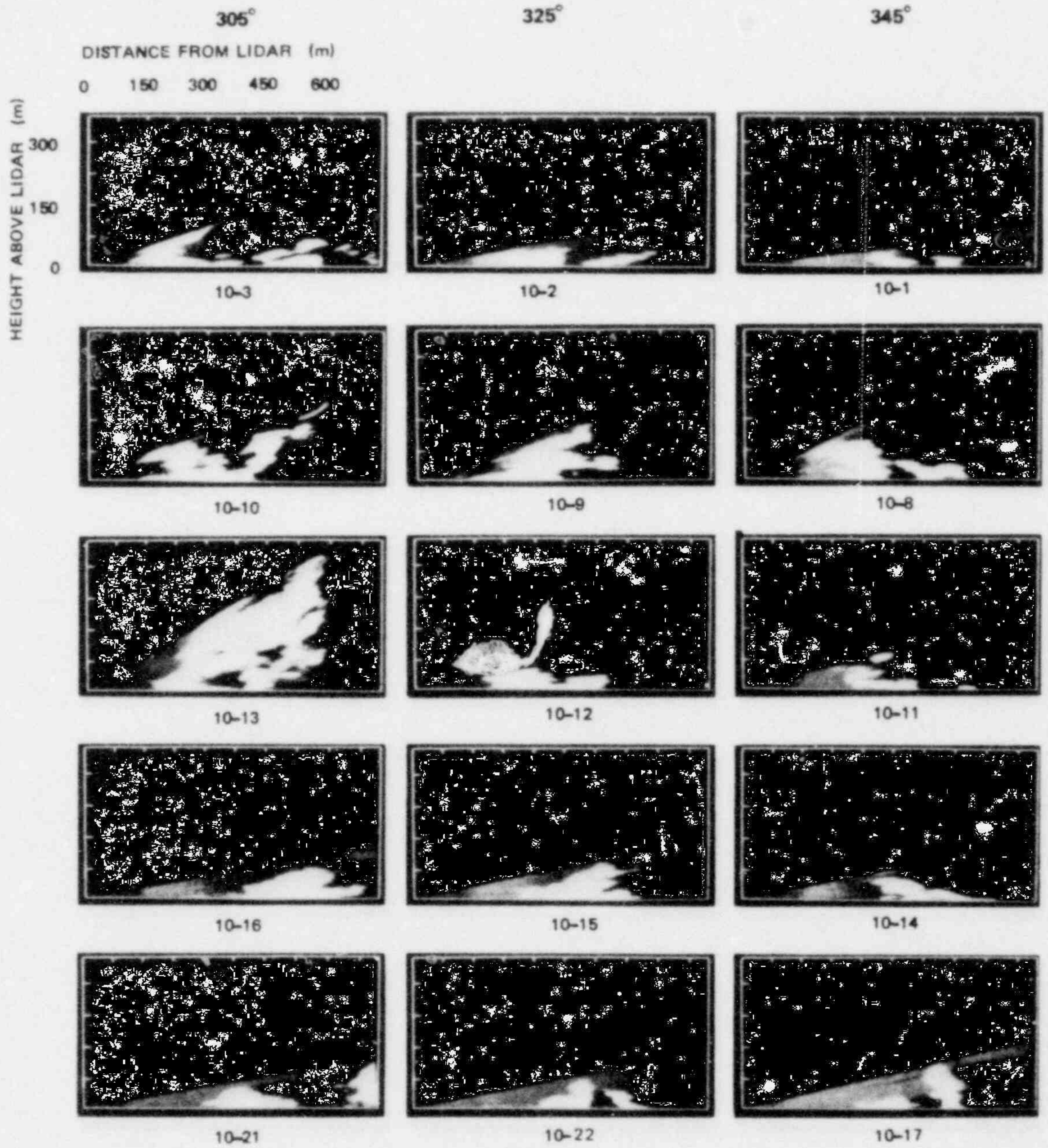

FIGURE 14 LIDAR VERTICAL CROSS SECTIONS OF TRACER SMOKE PLUMES RELEASED CONCURRENTLY NEAR THE EOCR BUILDING (PLUMES ON LEFT SIDE OF PICTURES) AND IN OPEN COUNTRY (PLUMES ON RIGHT SIDE OF PICTURES) FOR RUN 10

Scans at several lidar pointing (azimuth) angles are shown; the larger angles give data closer to the release points (see Figure 12).

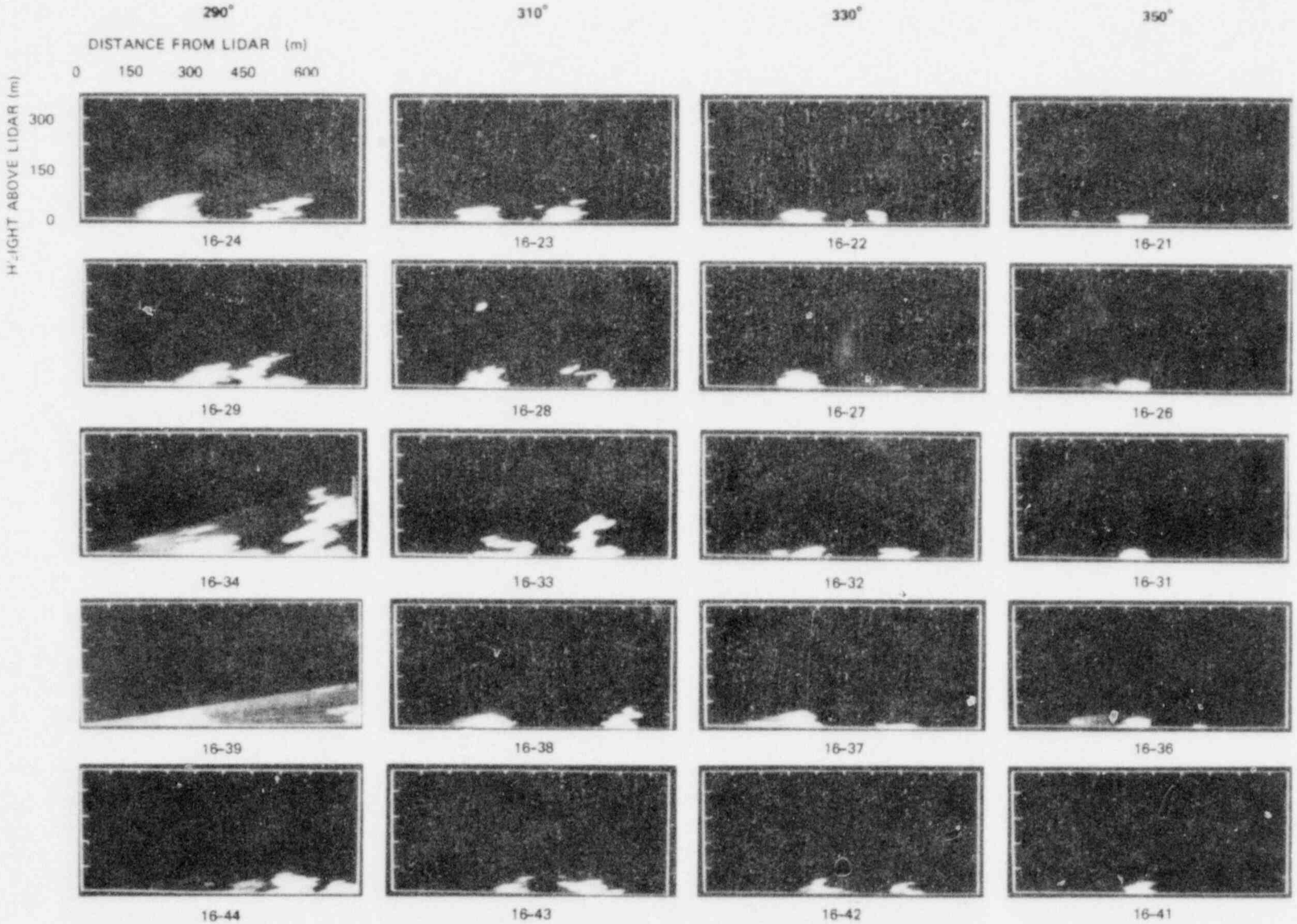

FIGURE 15 LIDAR VERTICAL CROSS SECTIONS OF TRACER SMOKE PLUMES RELEASED CONCURRENTLY NEAR THE EOCR BUILDING (PLUMES ON LEFT SIDE OF PICTURES) AND IN OPEN COUNTRY (PLUMES ON RIGHT SIDE OF PICTURES) FOR RUN 16

Scans at several lidar pointing (azimuth) angles are shown; the larger angles give data closer to the release points (see Figure 12).

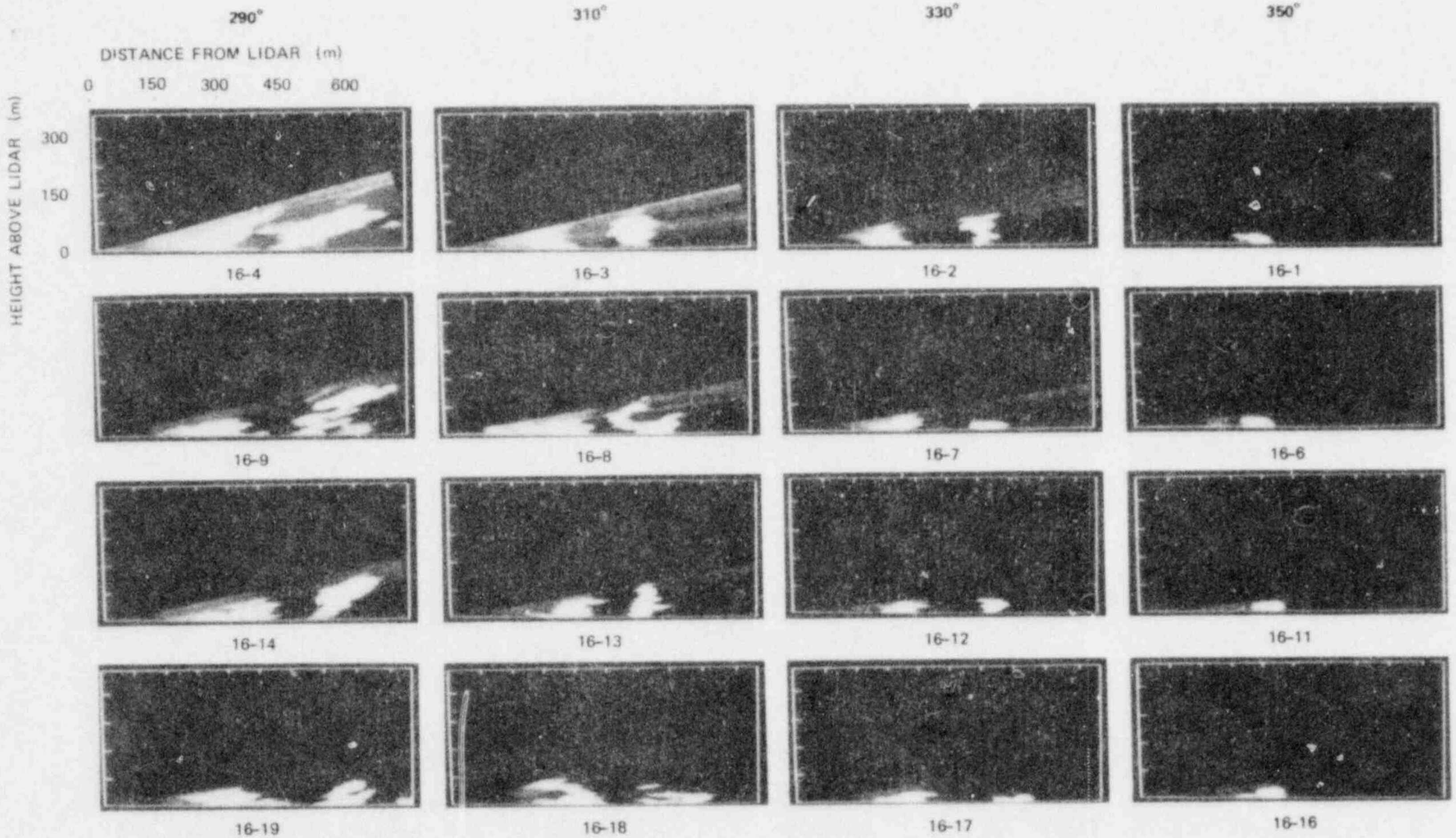

FIGURE 15 LIDAR VERTICAL CROSS SECTIONS OF TRACER SMOKE PLUMES RELEASED CONCURRENTLY NEAR THE EOCR BUILDING (PLUMES ON LEFT SIDE OF PICTURES) AND IN OPEN COUNTRY (PLUMES ON RIGHT SIDE OF PICTURES) FOR RUN 16 (Concluded)

Scans at several lidar pointing (azimuth) angles are shown; the larger angles give data closer to the release points (see Figure 12).

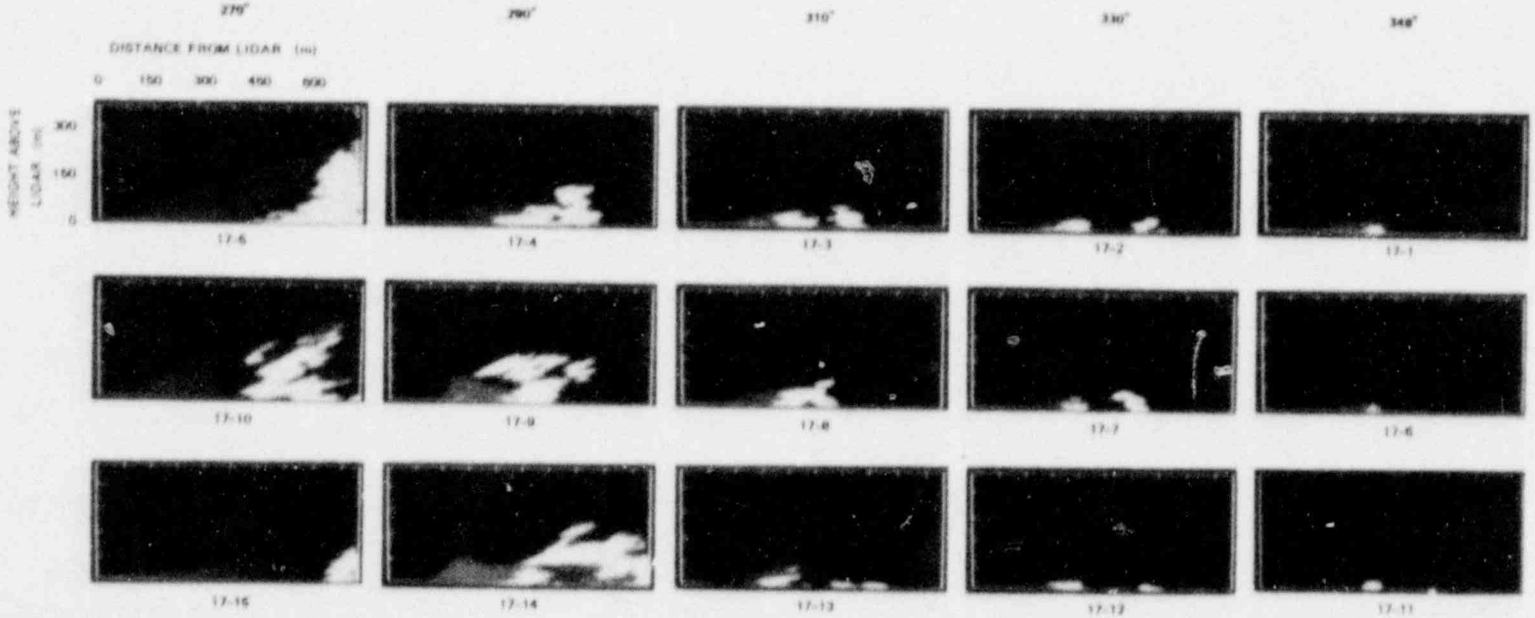

FIGURE 16 LIDAR VERTICAL CROSS SECTIONS OF TRACER SMOKE PLUMES RELEASED CONCURRENTLY NEAR THE EOCR BUILDING (PLUMES ON LEFT SIDE OF PICTURES) AND IN OPEN COUNTRY (PLUMES ON RIGHT SIDE OF PICTURES) FOR RUN 17

Scans at several lidar pointing (azimuth) angles are shown; the larger angles give data closer to the release points (see Figure 12).

POOR ORIGINAL

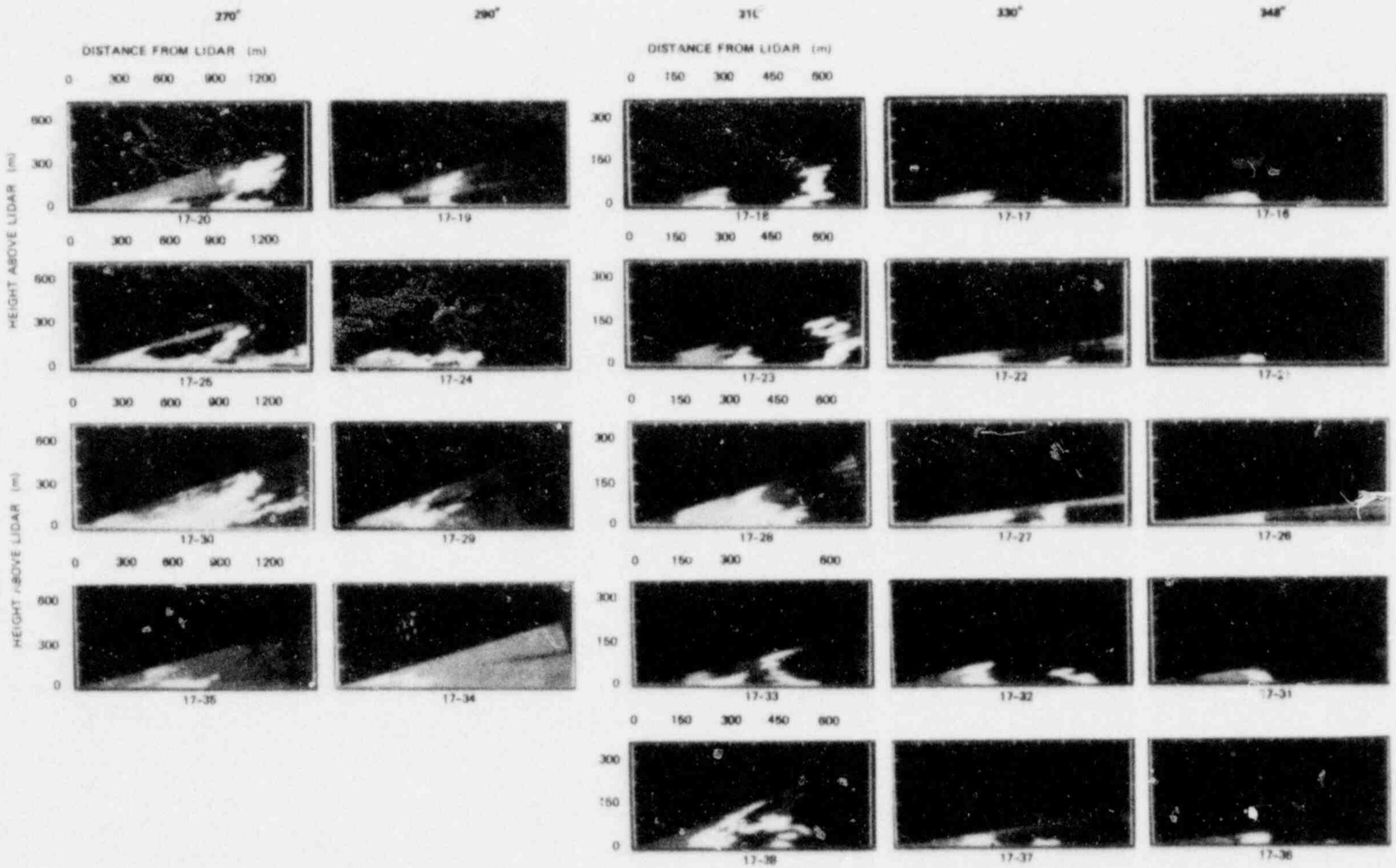

FIGURE 16 LIDAR VERTICAL CROSS SECTIONS OF TRACER SMOKE PLUMES RELEASED CONCURRENTLY NEAR THE EOCR BUILDING (PLUMES ON LEFT SIDE OF PICTURES) AND IN OPEN COUNTRY (PLUMES ON RIGHT SIDE OF PICTURES) FOR RUN 17 (Concluded)

Scans at several lidar pointing (azimuth) angles are shown; the larger angles give data closer to the release points (see Figure 12).

A value of F = 0, 1, or 2 was determined for each cross section by inspection. The resulting values of F are listed in Table 2 as a function of downwind distance, and the average values of F at each downwind distance are plotted in Figure 17. This figure shows that vertical dispersion is enhanced in the building wake for approximately 200 to 300 m downwind, which corresponds to 10 to 15 building heights. Such building effects on downwind dispersion are well known, and have been studied extensively; e.g., Halitsky (1966), Hatcher et al. (1978), Huber (1979), Johnson et al. (1975), Sagendorf et al. (1979), Start et al. (1977), Thompson and Lombardi (1977). Abbey (1976) reviewed many of these studies and described the NRC research program in this technical area.

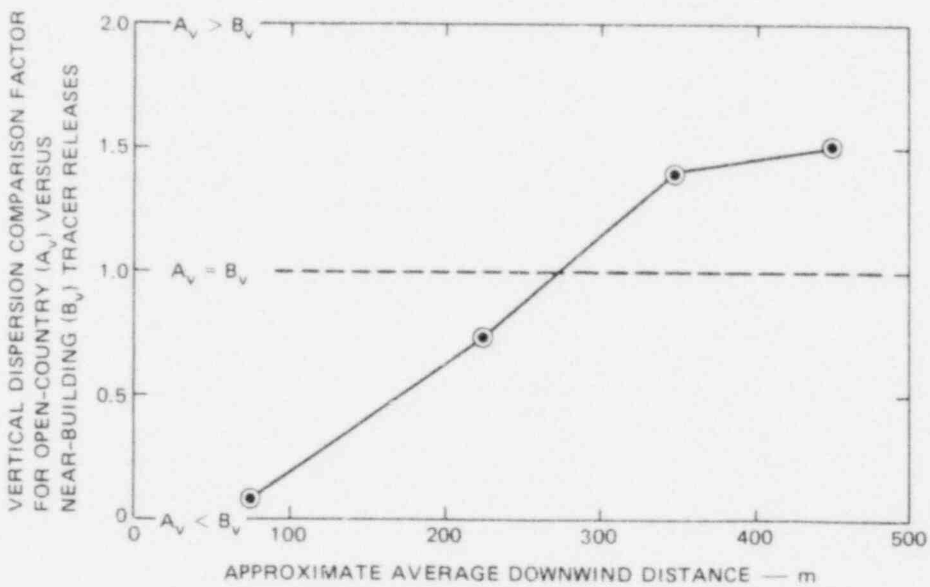

FIGURE 17 VERTICAL DISPERSION COMPARISON FACTOR AS A FUNCTION OF DOWNWIND DISTANCE

However, an unexpected result is the indication that beyond this 300-m distance, the vertical dispersion of the "open country" plume is greater than that of the building-influenced plume. Some of this effect is due to the geometrical distortion of the lidar viewing angles at progressively longer downwind distance, but overall it appears that the effect is real.

Possible explanations for this phenomenon could include persistent downward vertical motion in the building wake, and/or breakup of large ambient convective eddies by aerodynamically generated mechanical turbulence in the building wake. However, the qualitative results presented here are not definitive, and must be confirmed by other measurements before this finding can be considered to be established.

TABLE 2

VERTICAL DISPERSION COMPARISON FACTOR AS A FUNCTION OF DOWNWIND DISTANCE FOR THE VARIOUS LIDAR SCANS

Scan Nos. (First/Last)	Vertical Dispersion Comparison Factor at Indicated Downwind Distances*			
	50-100 m (Avg. 75m)	200-250 m (Avg. 225m)	300-400m (Avg. 350m)	400-500 m (Avg. 450)
11- 1/11- 4	0	2,2	2	
11- 5/11-8	0	0,2	1	
11- 9	0			
10- 1/10- 3	0	0	0	
10- 8/10-10	0	--**	--	
10-11/10-13	0	0	--	
10-14/10-16	0	--	--	
10-17/10-21	2	0	2	
16- 1/16- 4	0	2	2	2
16- 6/16- 9	0	0	2	2
16-11/16-14	0	1	2	2
16-16/16-19	0	0	0	0
16-21/16-24	0	0	1	1
16-26/16-29	0	0	1	2
16-31/16-34	0	1	2	2
16-36/16-39	0	0	2	--
16-41/16-44	0	1	1	0
17- 1/17- 5	0	2	2	2
17- 6/17-10	0	2	2	--
17-11/17-15	0	0	0	--
17-16/17-19	0	0	2	2
17-21/17-24	0	0	2	--
17-26/17-29	0	2	--	--
17-31/17-34	0	0	2	--
17-36/17-38	0	0	0	
Average Factor:	0.08	0.71	1.40	1.50

*The downwind distances listed correspond to the following lidar pointing (azimuth) angles for the various scans:

50 - 100m: 350-345°   300-400m: 315-305°
200 - 250m: 335-325°   400-500m: 290°

**The dashes indicate that the comparison factor cannot be determined, either because of missing data or because of merging of the two plumes.

V RECOMMENDATIONS FOR FURTHER WORK

The capability of the lidar technique to collect the large amount of data needed for quantitative diffusion analysis was experimentally demonstrated in the current study. However, digital processing of this data base was necessarily limited because of restrictions inherent in the two data processing methods currently available. Accordingly, an appropriate technique for processing of large data bases was developed and should be implemented so that the lidar can be used more effectively in further diffusion studies.

The proposed new data analysis method is diagrammed in Figure 18. It is designed to use, to the extent possible, existing hardware and software components of the Mark IX lidar data system. In the current method (see Figure 2), the lidar signatures are processed by the lidar PDP-11 computer using an overplot technique to convert the polar-scan data to an X-Y grid array, which is stored in a display memory. However, the current display memory does not permit accessing of these stored data by the PDP-11 computer.

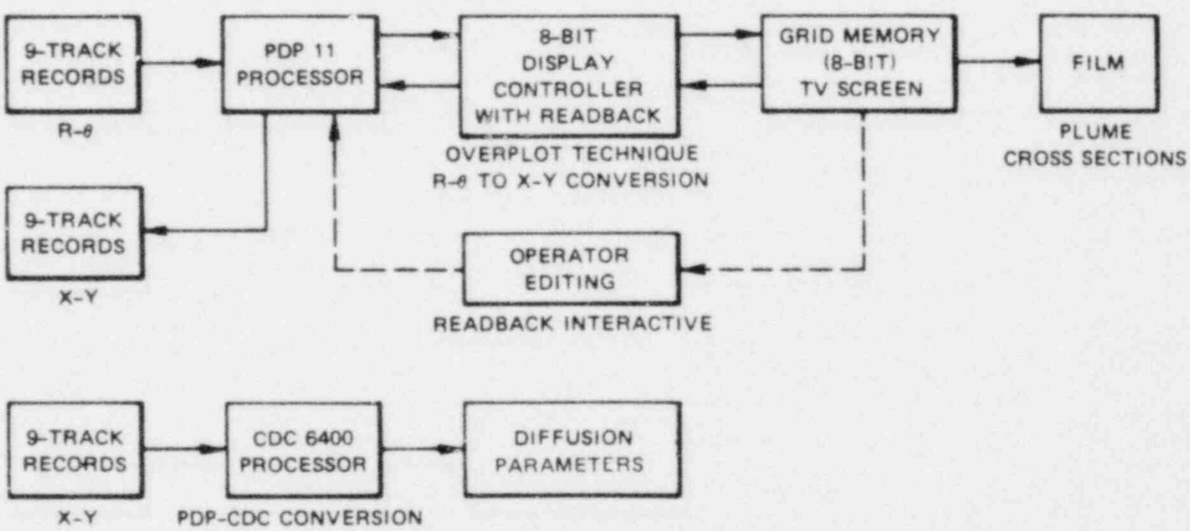

FIGURE 18 PROPOSED DATA ANALYSIS APPROACH RECOMMENDED FOR DIFFUSION PARAMETER COMPUTATION USING A LARGE LIDAR DATA BASE

In the proposed method, a new display memory with readback capabilities would be added so that the generated X-Y grid of numbers could be addressed by the computer. Therefore, the data as viewed on the TV display screen could be edited, and valid data in X-Y format could be written on a second tape drive controlled by the PDP-11 minicomputer. In addition, the data would be stored in their 8-bit form rather than the present 4-bit storage. Therefore, the full amplitude resolution provided by the 8-bit analog-to-digital converter used in the Mark IX lidar data system would be preserved in display memory.

The data tapes and gray-scale plume pictures processed with the new system would then be appropriate for transfer to other groups, if desired, for detailed diffusion analyses.

VI CONCLUSIONS

A technique for collecting a large lidar data base appropriate for analyzing diffusion parameters was developed and demonstrated. Although the data collection technique was successful, serious problems were encountered in developing a method for effectively analyzing these data. Use of the nine-track tape data recording medium reduced the amount of computer memory available for running analysis programs on the lidar minicomputer, and readdressing the file-structured nine-track magnetic tape was found to be significantly more time-consuming than readdressing the block-structured DECTAPE used previously.

As a result of these problems, an alternative methodology was developed for processing the data records on a larger computer system (CDC-6400). This approach has been shown to be feasible, but it is not suitable for analysis of large data bases for two reasons: (1) the large expense involved in converting tape formats and generating an X-Y grid of backscatter values, and (2) the lack of an appropriate display system driven by the large computer. After evaluating various computational techniques, defining data archiving requirements, and reviewing the latest available hardware technology, an improved method has now been formulated for processing and analyzing large lidar data bases for effective use in atmospheric diffusion studies. This method makes optimum use of both small- and large-computer techniques, and is described in detail in Section V of this report.

A two-week cooperative field program with NOAA/ARL-ID was conducted at the Idaho National Engineering Laboratory. Experiments were designed and conducted with the objective of utilizing the capabilities of lidar sensors to quantify diffusion parameters, especially in the vertical. Tracer smoke releases were made by the personnel of ARL-ID, and lidar backscatter data were collected by SRI using the Mark IX mobile lidar system. All data were successfully recorded on nine-track magnetic tape using a technique that provides for recording of 6000 lidar signatures without interruption. However, because of the problems discussed above, these data could only be processed to a limited extent by the lidar data system. All data were reduced to the form of lidar vertical cross sections depicting the two-dimensional structure of tracer smoke at various distances downwind of the source.

Because of the reasons just discussed, it was not feasible to analyze the lidar data in a detailed, quantitative manner. However, the distribution of tracer smoke observed for releases made simultaneously at sites near to and away from the EOCR reactor building provided data that could readily be analyzed qualitatively in terms of building wake effects. This qualitative analysis indicates that the presence of the building clearly enhances horizontal and vertical dispersion in the first 200 to 300 m of downwind travel. However, at downwind distances in the range of 300 to 500 m, there is some evidence that vertical dispersion is suppressed in the building wake relative to that of the open-country release. Possible explanations for this include persistent downdrafts in the building wake, and/or the breakup of ambient convective eddies by mechanical turbulence in the building wake.

REFERENCES

Abbey, R. F., Jr., 1975: "Atmospheric Dispersion Experiments Supported by ERDA and USNRC," Proceedings, 21st Annual Meeting of the American Nuclear Society, June 8-13, New Orleans, Louisiana.

Abbey, R. F., Jr., 1976: "Concentration Measurements Downwind of Buildings: Previous and Current Experiments," in Third Symposium on Atmospheric Turbulence, Diffusion, and Air Quality, October 19-22, 1976, Raleigh, North Carolina, American Meteorological Society, Boston, Massachusetts, pp. 247-254.

Collis, R. T. H. and E. E. Uthe, 1972: "Mie Scattering Techniques for Air Pollution Measurement with Lasers," Opto-Electronics, 4, pp. 87-99.

Halitsky, J., 1966: "Gas Diffusion Near Buildings," in Meteorology and Atomic Energy 1968, USAEC, TID-24180, pp. 221-255.

Hatcher, R. V., R. N. Meroney, J. A. Peterka, and K. Kothari, 1978: "Dispersion in the Wake of a Model Industrial Complex," NUREG-0373, U.S. Nuclear Regulatory Commission, available from National Technical Information Service, Springfield, Virginia 22161.

Huber, A. H., 1979: "An Evaluation of Obstacle Wake Effects on Plume Diffusion," in Fourth Symposium on Turbulence, Diffusion, and Air Pollution, January 15-18, 1979, Reno, Nevada, American Meteorological Society, Boston, Massachusetts.

Johnson, W. B., E. Shelar, R. E. Ruff, H. B. Singh, and L. Salas, 1975: "Gas Tracer Study of Roof-Vent Effluent Diffusion at Millstone Nuclear Power Station," SRI Project 3588, AIF/NESP-007b Atomic Industrial Forum, Washington, D.C., 295 pp.

Sagendorf, J. F., N. R. Ricks, G. E. Start, and C. R. Dickson, 1979: "Near Building Diffusion Determined from Atmospheric Tracer Experiments," in Fourth Symposium on Turbulence, Diffusion, and Air Pollution, January 15-18, 1979, Reno, Nevada, American Meteorological Society, Boston, Massachusetts, pp. 596-602.

Start, G. E., J. H. Cate, C. R. Dickson, N. R. Ricks, G. R. Ackerman, and J. F. Sagendorf, 1977: "Rancho Seco Building Wake Effects on Atmospheric Diffusion," NOAA Technical Memorandum ERL-ARL-69, Environmental Research Laboratories Air Resources Laboratories, NOAA, Idaho Falls, Idaho, 185 pp.

Thompson, R. S. and D. J. Lombardi, 1977: "Dispersion of Roof Top Emissions from Isolated Buildings: A Wind Tunnel Study," EPA-600/4-77-066, U.S. Environmental Protection Agency, Research Triangle Park, North Carolina.

Uthe, E. E., and K. J. Allen, 1975: "A Digital Real-Time Lidar Data Recording, Processing, and Display System," J. Optical and Quantum Electronics, 7, 121-129.

Uthe, E. E., and W. B. Johnson, 1976: "Lidar Observations of Plume Diffusion at Rancho Seco Generating Station," Final Report, SRI Project No. 4617, EPRI NP-238, (SOA 75-316), Electric Power Research Institute, Palo Alto, California 94304.

Uthe, E. E., W. B. Johnson, and H. Till, 1979: "Vertical Plume Diffusion Parameters Derived by Lidar for the Rancho Seco Generating Station," in Fourth Symposium on Turbulence, Diffusion, and Air Pollution, January 15-18, 1979, American Meteorological Society, Boston, Massachusetts 02108, pp. 536-540.

Appendix

LIDAR EQUIPMENT AND TECHNIQUES

1. Lidar Equipment

The SRI Mark IX mobile lidar system was designed for use on environmental programs that require observations at relatively short ranges (0 to 10 km) with a high data rate and sufficient transmitter energy for single-pulse signature analysis. The configuration of the lidar van and its equipment is pictured in Figure A-1. Additional specifications are provided in Table A-1.

The laser transmitter and receiver optics and detector are mounted on a pointable pedestal with elevation and azimuth drive motors for automatic scanning capabilities. The detector may be gated in a time-squared fashion to correct for the inverse-range squared dependence and may be logarithmically amplified to effectively observe backscatter signals over four orders of magnitude. The system is equipped with two complete and independent real-time data recording, processing, and display subsystems. The analog video-disk subsystem was introduced in 1970 and has been used by Johnson et al. (1973) to obtain electronically-generated pictorial displays of plume structure from a time series of lidar signatures. However, because of the relatively low bandpass capabilities of the disk recorder and nonlinear transfer functions of the supporting electronics, the disk records are not satisfactory for quantitative density analysis. A computer-based digital system that solves the problems associated with the analog system was developed in 1973 and has been discussed in a journal publication by Uthe and Allen (1975). Pictorial displays with 16 gray levels can be generated, with picture brightness linearly related to backscatter intensity. In addition, digital records are available for computer processing in terms of quantitative optical or physical densities and for profile analysis as applied in this study.

2. Sampling Configuration

For the application described in this report, the lidar van was positioned to enable the Mark IX lidar to fire through the plume to be sampled and the intervening clear-air region between the van position and the plume, as illustrated schematically in Figure A-2(a). A pulse of energy is fired along a sampling path and the quasi-continuous backscattered energy is sampled at a time interval, Δt, that, given the speed of light, translates to a range interval ΔR along the sampling path. The location of any backscatter sample is thus known as a function of range along the sampling path and the known elevation angle of that path. A vertical cross-sectional sampling of the plume is obtained by incrementing the elevation angles of the individual sampling paths by a known amount, $\Delta\theta$, thus providing a two-dimensional array of samples in polar format as indicated by the dots in Figure A-2(a).

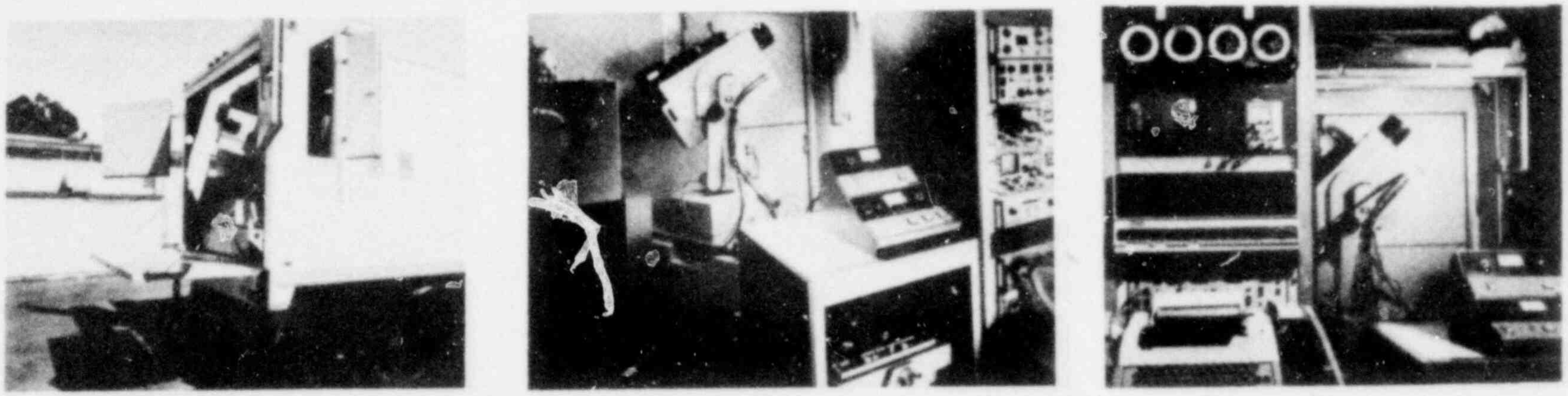

(a) MARK IX LIDAR VAN

(b) ANALOG DATA AND FIRE CONTROL ELECTRONICS

(c) DIGITAL DATA ELECTRONICS AND TV DISPLAY

EXTERIOR AND INTERIOR VIEWS OF THE LIDAR VAN

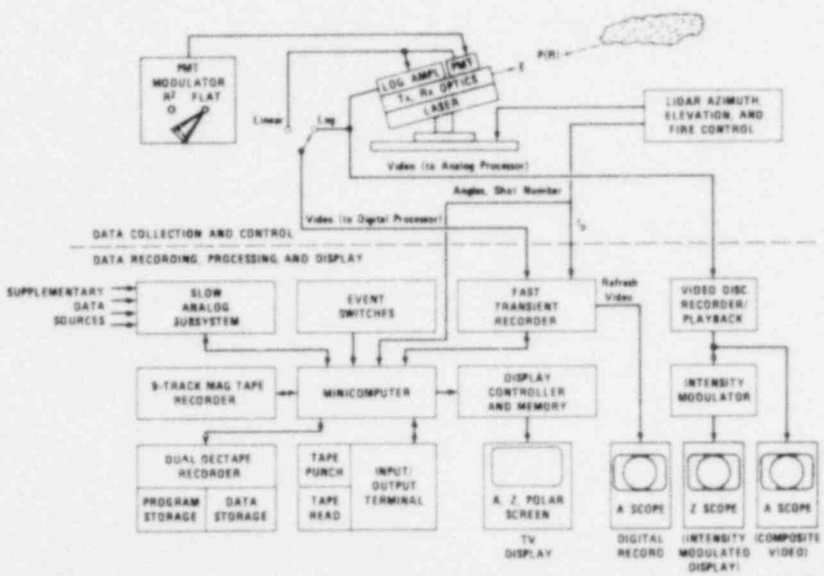

BLOCK DIAGRAM OF THE LIDAR SYSTEM

LIDAR SPECIFICATIONS

TRANSMITTER

6943Å Wavelength
0.5 mrad Beamwidth
1.0 J Pulse Energy
30 ns Pulse Length
60 ppm Maximum PRF

RECEIVER

6 inch Newtonian
1 to 5 mrad Field of View
5Å Predetection Filter
RCA 7265 PMT Detector
4-decade, 35-MHz Logarithmic Amplifier. Inverse-range-squared or step-function PMT modulation.

DATA SYSTEMS

Analog video disc recording (4.5 MHz) with A-scope and Z-scope real-time displays. Digital magnetic tape (data and programs) recording (25 MHz) with computer processing and real-time TV display (512 x 256 x 4 bit) of processed data.

MOUNT

Automatic azimuth and elevation fire and scan with 0.1° minimum resolution. Automatic reset. Mechanical safety stops.

TA-653583-311

FIGURE A-1 THE SRI MARK IX MOBILE LIDAR SYSTEM

Table A-1

MARK IX LIDAR SPECIFICATIONS

Item	Description
Transmitter	
Laser rod	Ruby (3/8 × 3 inches)
Wavelength (Å)	6943.0 ± 0.4
Beamwidth (mrad)	< 1
Optics	4-to-1 Galilean beam expander and 2-inch mirror coaxial with receiver telescope
Pulse energy (joules)	1.0
Pulse length (ns)	30
Q-switch	Pockets cell
Maximum PRF (pulses/min)	60
Cavity cooling	Refrigerated water
Receiver	
Optics	Newtonian reflector (6 inches)
Field-of-view (mrad)	1.0 to 5.5
Predetection filter passband width (Å)	3 to 5 (thermally controlled)
Detector	RCA 7265 PMT (S-20 photocathode)
Video amplifiers	Log (4 decades, 35 MHz) and/or wideband linear
PMT even-numbered dynode modulation	
Gain compensation	Inverse range squared correction or flat (selectable by front-panel control)
PMT 'on' period	1 μs (150 m), 10 μs (1.5 km), 100 μs (15 km), 200 μs (30 km), or variable
Prefull 'on' control:	
(a) Step gain (dB down)	0 dB, -10 dB, -20 dB, -30 dB or -40 dB
(b) Delay from lase	0, 5 μs (750 m), 10 μs (1.5 km), 20 μs (3 km), 30 μs (4.5 km), or variable
Scanning and firing	
Azimuth and elevation (degree/shot)	0.1, 0.2, 0.5, 1.0, 2.0, 5.0, or 10, or by external programmer
Firing rate (PPM)	1, 2, 3, 4, 5, 10, 20, 30, or 60 plus variable (120 PPM available for playback)
Digital processing/recording/display (25-MHz system)	
A/D conversion	Resolution: 8 bits Bit rate: 500 Mb/s (max)
Sample intervals (range resolution)	0.01 μs (1.5 m), 0.02 μs (3 m), 0.05 μs (7.5 m), 0.1 μs (15 m), 0.2 μs (30 m), 0.5 μs (75 m), 1 μs (150 m), and so on to 10 s (Mixed time base allows increased resolution at range of aerosol of interest.)

Table A-1

MARK IX LIDAR SPECIFICATIONS
(Concluded)

Item	Description
Total number of samples per lidar shot:	
• Recorded	Selectable 2048, 1024, 512, or 256
• Displayed	512 (Sequential, every 2nd or every 4th sample)
Programmable delay (from lase)	In 10-sample increments
Displays:	
• Scope (from refresh memory)	Amplitude versus range, continuously refreshed between lidar shots
• TV (90 rotated)	• Height or range versus time -- Y-axis (elements): 512 samples -- X-axis (lines): 256 lidar shots -- Z-axis (intensity modulated): 16-level grey scale • Amplitude versus range
Computer memory size	16K-words (16-bits/word)
Programs	RT-11/BASIC; RT-11/FORTRAN IV, various lidar programs (log-amplitude, inverse-range-squared correction, cloud and aerosol density inferences, and so on).
Peripherals	Magnetic tape storage; teletype terminal with paper tape punch/reader
Analog processing/recording/display (4.5-MHz system)	
Data storage	Video disk with READ BETWEEN WRITE capabilities (72,000 lidar shots per disc)
Data recording	Polaroid or 35-mm film
Scope displays	
• Intensity modulated (z-scope)	• READ BETWEEN WRITE--progressive buildup of time or distance traveled as a function of height or range • Playback: -- Cartesian coordinates: X-axis--time or distance traveled Y-axis--height or range Z-axis--intensity (function of signal strength) -- Polar coordinates: r--range ϕ--degrees stepped between shots
• Standard (A-scope)	• Single shot: -- Log amplitude versus range (time) -- Linear amplitude versus range • Composite of up to 360 shots (both log and linear as above)
Frequency response	• Using video disc storage: 4.5 MHz • Direct on film through log amplifier: 35 MHz • Direct on film without log amplifier: 100 MHz

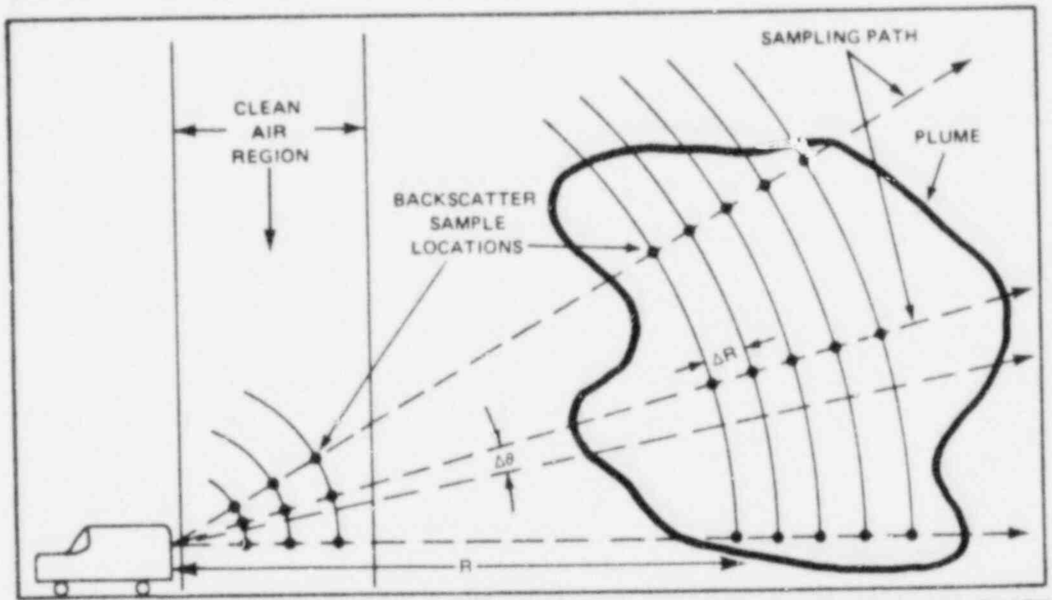

(a) SCHEMATIC REPRESENTATION OF PLUME AND CLEAR AIR SAMPLING BY LIDAR BACKSCATTER

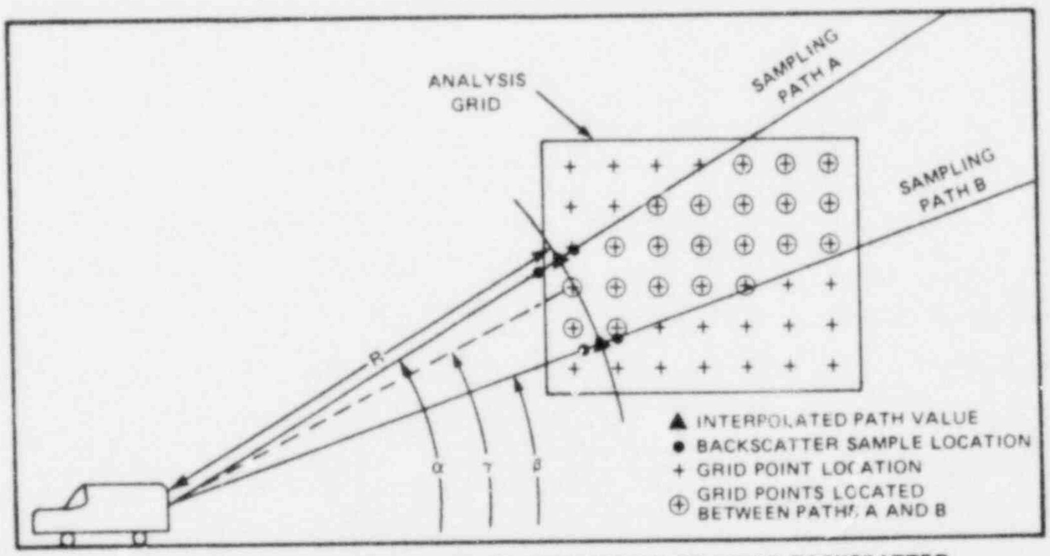

(b) SCHEMATIC REPRESENTATION OF CONVERSION OF LIDAR BACKSCATTER DATA FROM POLAR TO RECTANGULAR FORM

FIGURE A-2 LIDAR SAMPLING CONFIGURATION AND DATA FORMATS

3. Data Formatting

In order to analyze the lidar data computationally, a rectangular rather than a polar array was desired. Such an array can be provided by specifying an analysis grid of rectangular point locations as illustrated in Figure A-2(b) and interpolating the polar array to obtain values at the grid points. The interpolation scheme employed consisted of the following process:

- Grid points lying between two sampling paths are identified.
- For each such grid point, a backscatter value is obtained on each bracketing path, at the same range (R) as the grid point, by linearly interpolating the sample values along the path.
- The path values thus obtained are then interpolated to the grid squares in question by an angular interpolation along the arc representing range R.

4. Data Normalization

In its initial form, the analysis array consists of backscatter ratio quantities, S, in decibel form:

$$S = 10 \log_{10} (\beta_p + \beta_c) ,$$

where β_p and β_c are the backscatter components from the smoke plume and the clear air, respectively. The values of S can also be converted to a linear ratio of β_p to β_c by the following process:

- Designate the backscatter from clear air alone in the form

$$S_c = 10 \log_{10} \beta_c .$$

- Determine the value S_c from backscatter samples in the clear air region [see Figure A-2(a)] and use this value to write an expression for the ratio of total to clear air backscatter in decibel form as

$$S_p = 10 \log_{10} (\beta_p + \beta_c) - 10 \log_{10}(\beta_c) .$$

- Rewrite above equation in the form

$$S_p = 10 \log_{10}\left(\frac{\beta_p}{\beta_c} + 1\right) ,$$

which in turn may be written as

$$\frac{\beta_p}{\beta_c} = 10^{0.1S_p} - 1.$$

In this way a rectangular array of values for the linear backscatter ratio, D, can be obtained for analysis, where

$$D = \frac{\beta_p}{\beta_c} .$$

5. Contour Analysis

Using the retangular array of decibel (S_p) values* described above, a contour analysis can be performed on each array by means of an objective, computerized contouring routine available on the SRI computer system. Suitable contour intervals can be chosen so that the resulting map illustrates the two-dimensional distribution of density in the vertical cross section through the smoke tracer plume.

6. Distributional Analysis

For comparison with the Gaussian model currently in use, it is generally of interest to investigate the horizontal and vertical density distributions and their statistics. The lidar data consist of two-dimensional arrays of backscatter-ratio (plume-density) values; we normally average over one dimension in order to compute the density distribution with respect to the second dimension. Thus, our analysis provides vertically averaged plume density as a function of horizontal distance along the lidar sampling path, and horizontally averaged plume density as a function of height above the lidar path. The density distributions thus computed can be fitted with Gaussian curves using mean, maxima, and standard deviations (σ) computed from the data in the distributions themselves. The approach to fitting field data with a Gaussian function is not straightforward since the data exhibit varying distributions and the method of producing the most representative Gaussian fit is thus somewhat arbitrary. Four methods are available as

---

*Use of logarithmic values avoids crowding of contours.

possible choices in current practice. The first of these involves fitting by a Gaussian distribution in which the backscatter ratio average $\overline{D}$ is calculated as

$$\overline{D} = \overline{D}_{max} \exp - \frac{(x - \overline{x})^2}{2\sigma^2} ,$$

where $|x - \overline{x}|$ is the distance between the location of specific $\overline{D}$ values and their mean location. In applying the procedure, a best estimate is made of the parameters $\overline{x}$ and σ, and the best fit values are then determined by a nonlinear least-squares process developed by Marquart (1963).

The three other methods are given by Pooler (1979) and consist of

- A direct method in which standard deviation is computed from the data in the conventional statistical manner

$$\sigma = \sqrt{\overline{(x-\overline{x})^2}} .$$

- An equal area method in which σ values are determined as those which divide the area under the given density distribution curve into the percentage of total area specified by the Gaussian function; that is

$$\frac{\int_{-\infty}^{x_1} \overline{D}\, dx}{\int_{-\infty}^{+\infty} \overline{D}\, dx} = 0.1587 ,$$

and

$$\frac{\int_{-\infty}^{x_2} \overline{D}\, dx}{\int_{-\infty}^{+\infty} \overline{D}\, dx} = 0.8413 ,$$

where x is distance.

- A maximum value method in which σ's are calculated by assuming that the Gaussian distribution fitting the data has the same maximum value and total area under the density curve as do the sample data. Since the maximum value of $\overline{D}$ in a Gaussian distribution would be given by

$$\overline{D}_{max} = \frac{\int_{-\infty}^{+\infty} \overline{D}\,dx}{\sqrt{2\pi}\,\sigma} ,$$

the value of σ can be computed as

$$\sigma = \frac{\int_{-\infty}^{+\infty} \overline{D}\,dx}{\sqrt{2\pi}\,\overline{D}_{max}} .$$

Vertical and horizontal density distributions of $\overline{D}$ from the Duane Arnold project (Thuillier and Mancuso, 1980) were fit by each of the four methods described above and the results compared. The nonlinear least-squares (NLLS) fit appeared to be consistently superior to the others from the visual appearance of the fits and also had the lowest root-mean-square error (RMSE). The equal-area method (EAM) was nearly as satisfactory as the NLLS method. Neither of the remaining two methods was at all satisfactory.

In view of this comparative test, the Duane Arnold data were fit with Gaussian parameters estimated on the basis of NLLS.

REFERENCES

Marquart, D. W., 1963: "An Algorithm for Least Squares Estimation of Parameters," J. Soc. Indust. Appl. Math., 11(2), pp. 431-441.

Pooler, F., 1979: "Methodology to Estimate Sigmas from STATE Data," EPA Internal Memorandum.

Thuillier, R. H. and R. L. Mancuso, 1980: "Building Effects on Effluent Dispersion from Roof Vents at Nuclear Power Plants," Final Report, SRI Project No. 6888, EPRI NP-1380, (Project 1073-1), Electric Power Research Institute, Palo Alto, California 94304.

NRC FORM 335 (7-77) U.S. NUCLEAR REGULATORY COMMISSION

BIBLIOGRAPHIC DATA SHEET

1. REPORT NUMBER (Assigned by DDC): NUREG/CR-1835

4. TITLE AND SUBTITLE (Add Volume No., if appropriate)
Application of Lidar Techniques to Estimating Atmospheric Dispersion

2. (Leave blank)

3. RECIPIENT'S ACCESSION NO.

7. AUTHOR(S)
E. E. Uthe and W. B. Johnson

5. DATE REPORT COMPLETED
MONTH: November YEAR: 1980

9. PERFORMING ORGANIZATION NAME AND MAILING ADDRESS (Include Zip Code)
SRI International
333 Ravenswood Avenue
Menlo Park, California 94025

DATE REPORT ISSUED
MONTH: December YEAR: 1980

6. (Leave blank)

8. (Leave blank)

12. SPONSORING ORGANIZATION NAME AND MAILING ADDRESS (Include Zip Code)
Site Safety Research Branch
Division of Reactor Safety Research
Office of Nuclear Regulatory Research
U.S. Nuclear Regulatory Commission
Washington, D.C. 20555

10. PROJECT/TASK/WORK UNIT NO.

11. CONTRACT NO.
FIN B6222
NRC-04-77-147

13. TYPE OF REPORT
Final Report

PERIOD COVERED (Inclusive dates)
8/77 - 11/80

15. SUPPLEMENTARY NOTES

14. (Leave blank)

16. ABSTRACT (200 words or less)

A new technique for collecting a large lidar data base appropriate for analyzing atmospheric diffusion parameters was developed, along with a new method for processing lidar data records on a large computer system (CDC-6400).

To test these new techniques, a two-week cooperative field program was conducted at the Idaho National Engineering Laboratory. Tracer gas and smoke releases were made by the National Oceanic Atmospheric Administration Air Resources Laboratory (NOAA/ARL), and lidar backscatter data were collected by SRI using the Mark IX mobile lidar system. All lidar data were reduced to the form of vertical cross-sections depicting the two-dimensional structure of tracer smoke at various distances downwind of the source.

Analysis of the measured distributions of tracer smoke indicates that the presence of the building clearly enhances horizontal and vertical dispersion in the first 200 to 300 m of downwind travel. However, at downwind distances in the range of 300 to 500 m there is some evidence that vertical dispersion is suppressed in the building wake relative to that of the open-country release.

17. KEY WORDS AND DOCUMENT ANALYSIS

17a. DESCRIPTORS

17b. IDENTIFIERS/OPEN-ENDED TERMS

18. AVAILABILITY STATEMENT
Unlimited

19. SECURITY CLASS (This report)
Unclassified

21. NO. OF PAGES

20. SECURITY CLASS (This page)
Unclassified

22. PRICE
$